Tidal Dissipation in Stars and Giant Planets

Gordon I. Ogilvie

Department of Applied Mathematics and Theoretical Physics, University of Cambridge, Cambridge CB3 0WA, United Kingdom; email: gio10@cam.ac.uk

Annu. Rev. Astron. Astrophys. 2014. 52:171–210

The *Annual Review of Astronomy and Astrophysics* is online at astro.annualreviews.org

This article's doi:
10.1146/annurev-astro-081913-035941

Keywords

celestial mechanics, fluid dynamics, internal waves, binary stars, extrasolar planets, giant planets: satellites

Abstract

Astrophysical fluid bodies that orbit close to one another induce tidal distortions and flows that are subject to dissipative processes. The spin and orbital motions undergo a coupled evolution over astronomical timescales, which is relevant for many types of binary star, short-period extrasolar planetary systems, and the satellites of the giant planets in the Solar System. I review the principal mechanisms that have been discussed for tidal dissipation in stars and giant planets in both linear and nonlinear regimes. I also compare the expectations based on theoretical models with recent observational findings.

1. INTRODUCTION

Body 1: the body in which the tide is raised

Body 2: the body that raises the tide

The orbital motion of a gravitating system of extended fluid bodies, such as stars and giant planets, differs from that of a set of point masses. They are nonspherical as a result of both their rotation and their tidal deformation due to the nonuniform gravitational attraction of their companions. In a Newtonian system of two such bodies, the Keplerian orbital elements evolve in time. The largest effects are nondissipative in character and include orbital precession. Of greater interest and subtlety is the irreversible evolution of the size and shape of the orbit driven by dissipative processes.

The study of tides has a long and fascinating history (Cartwright 1999, Deparis et al. 2013). It involves an interesting combination of celestial mechanics, which is nontrivial but can be explored relatively easily, and fluid dynamics, which involves some deeper physical issues that are touched on in this article. Indeed, this review is devoted to stars and giant planets, which are wholly or predominantly fluid, rather than terrestrial bodies, which are predominantly solid, although deformable. In other words, our interest is in fluid dynamics rather than solid mechanics, in which the dissipative properties have a different nature. However, there is not a clean separation between these areas. Neutron stars have solid crusts, giant planets may contain solid cores, and terrestrial bodies may contain oceans and atmospheres with important tidal phenomena. In the case of Earth, a fluid layer that is only 0.023% of the planet's mass dominates the tidal dissipation.

Our focus is also on purely gravitational tides, which can be regarded as a subset of interactions between neighboring astrophysical bodies. Thermal and magnetic tides are also possible, in which one body affects the other in a way that is not spherically symmetric and may depend periodically on time owing to the spin and orbital motion. As for gravitational tides, both wave-like and nonwave-like disturbances may be generated.

A useful dimensionless parameter that can be taken as a simple estimate of the tidal deformation of one body by another is the tidal amplitude parameter $\epsilon = (M_2/M_1)(R_1/d)^3$, where M_1 and M_2 are the masses of the two bodies, R_1 is the (mean) radius of body 1 and d is the orbital separation (**Figure 1**). This is a measure of the ratio, at the surface of body 1, of the tidal gravity due to body 2, GM_2R_1/d^3, to the gravity of body 1 itself, GM_1/R_1^2; it is also an estimate of the ratio of the height of the tide compared with the radius of body 1.

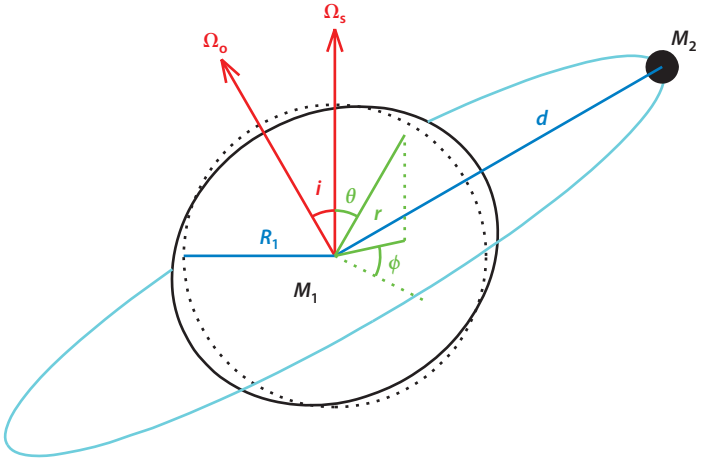

Figure 1

Geometry of tidal interaction. When considering the tide raised in body 1 by body 2, it is convenient to use spherical polar coordinates (r, θ, ϕ) centered on body 1 and aligned with its rotation axis. Ω_s and Ω_o are the spin and orbital angular velocity vectors, respectively. The figure represents the tidal bulge but not the rotational bulge.

Tidal interactions are therefore strongly dependent on the separation of the bodies in comparison with their sizes. The most familiar example (although beyond the scope of this review) is of course the Earth-Moon system, in which the Sun also plays a significant role. Tidal dissipation on Earth leads to a lengthening of both the day and the month as angular momentum is transferred from the planetary spin to the orbit. Tidal evolution, including the effects of tidal dissipation in giant planets, has been similarly influential for many of the regular satellites of the other planets in the Solar System (Peale 1999). Tidal interactions have many applications to binary stars, including pre-main-sequence, main-sequence, giant, and degenerate stars, whenever the ratio of orbital separation to stellar radius is sufficiently small. Much recent work on tides has been stimulated by the discovery since 1995 of numerous extrasolar planets that orbit very close to their host stars, and also by the prospect of detecting gravitational radiation from merging double-degenerate binary stars, in which tidal effects may alter the predicted wave signals (e.g., Kochanek 1992, Bildsten & Cutler 1992).

Tidal torque: the rate of transfer of (axial) angular momentum from the orbit to the spin of body 1

In this review we concentrate on situations in which the tidal amplitude parameter $\epsilon \ll 1$, although important internal nonlinearities may still be present, as discussed in Section 4. (There are of course more extreme situations in which the body is tidally disrupted, resulting in a significant loss of mass; this includes Roche-lobe overflow in binary stars with circular orbits and the tidal disruption of stars on eccentric orbits around the black hole at the center of a galaxy, or of planets scattered close to their host stars, e.g., Guillochon et al. 2011). For the giant planets of the Solar System, the largest values of ϵ are approximately 2×10^{-7} (Jupiter, due to Io), 3×10^{-8} (Saturn, due to Titan), 4×10^{-8} (Uranus, due to Ariel), and 8×10^{-8} (Neptune, due to Triton). Among exoplanetary systems confirmed so far, the largest values are approximately 2×10^{-4} for the tide in a star (WASP-18; Hellier et al. 2009) and 6×10^{-2} for the tide in a planet (WASP-19 b; Hebb et al. 2010). The tides in giant planets forced by small satellites and by nearby host stars may be in very different regimes, which motivates a study of linear and nonlinear tides.

The dominant tidal interaction is usually between the gravitational quadrupole moment of one body and the monopole moment of the other. The second body can then be thought of as a point mass, whereas the first is endowed with an ellipsoidal bulge (**Figure 1**). The monopole field of body 2 varies over the volume occupied by body 1, creating a tidal field that is aligned with the axis joining the centers of the bodies. This tidal field deforms body 1, generating a quadrupole moment. In the simplest case a spheroidal bulge arises, aligned with the axis, which gives rise to an attractive net force in that radial direction.

The process of deformation involves fluid dynamics, as discussed in detail later in this review, and is generally accompanied by dissipation. As a result, the quadrupole moment of body 1 is not instantaneously related to the tidal field and is not generally aligned with the radial direction. This effect is often modeled crudely by allowing for a certain time lag in the response. The dissipative part of the net force between the bodies has two aspects. One is that the radial force is retarded and therefore resists the oscillatory radial motion associated with any eccentricity of the orbit. The other is that an angular force arises that resists the relative angular motion associated with any inequality of the spin and orbital angular velocity vectors. This force also gives rise to a tidal torque that couples the spin and orbit, allowing an exchange of angular momentum. Both forces are resistive in nature and are accompanied by dissipation of energy.

The responses of spin and orbit to changes in angular momentum are different. Although spin angular momentum increases with angular velocity, orbital angular momentum decreases, which can lead to paradoxical behavior. The tidal torque seeks to equalize the spin and orbital angular velocity vectors through an exchange of angular momentum and the dissipation of energy. In many cases the spin moment of inertia is much smaller than the orbital moment of inertia, and the first effect of tidal dissipation is a tendency toward equalization of the spin and orbital angular velocity

vectors, involving only a small change in the orbit. In the case of a circular orbit this means both synchronization of the spin with the orbit and alignment of the spin axis with the orbit normal, with the final angular velocity vector being determined by the total angular momentum. If the orbit is eccentric, however, then the orbital angular velocity is not constant and there is a tendency toward pseudosynchronization, i.e., spin at a rate close to, but slightly less than, the instantaneous orbital angular velocity at the pericenter, where the tidal interaction is strongest (Hut 1981).

Obliquity: the angle between the rotation axis of body 1 and the orbit normal; also known as the spin-orbit misalignment

Tidal equilibrium: a double synchronous state in which two bodies have a circular orbit with synchronized, aligned spins and no further tidal evolution occurs

Both the radial force and the tidal torque contribute to the evolution of eccentricity, which can either increase or decrease as a result. Similarly, the obliquity, which is the angle between the spin and orbital angular momentum vectors, can either increase or decrease. Circularization and spin-orbit alignment may be regarded as the normal outcomes of tidal dissipation; in order to increase e or i, the energy source associated with an asynchronous spin is needed. This possibility is discussed in more detail in Section 2.3 below.

In most binary stars the theoretical endpoint of tidal evolution, if other processes such as magnetic braking, gravitational radiation, and stellar evolution are ignored, is a tidal equilibrium or double synchronous state, in which both stars are in aligned, synchronous rotation with a circular orbit, as occurs with Pluto and Charon. There is then only a static tidal deformation and no dissipation. (However, internal processes such as convection and meridional circulation may induce a differential rotation in the stars, which would imply ongoing tidal dissipation.) The double synchronous state has not yet been verified observationally for a binary star. Two candidates can be found in Meibom et al. (2006, their table 1), although in each binary only one spin period and neither obliquity is measured. Albrecht et al. (2007) give the first observations of both stellar obliquities (consistent with zero) in a main-sequence binary, but the orbit is eccentric.

In systems of extreme mass ratio, however, such as the satellite systems of the giant planets and many short-period extrasolar planetary systems, this endpoint cannot be reached. Tidal equilibria may be characterized by their angular velocity Ω. The total angular momentum $L(\Omega)$ of a tidal equilibrium is the sum of the spin and orbital contributions, $L_s(\Omega)$ and $L_o(\Omega)$, which are increasing and decreasing functions, respectively, such that $L(\Omega)$ has a minimum, critical value L_c at $\Omega = \Omega_c$. If $L < L_c$, then no tidal equilibrium is accessible. If $L > L_c$, then two such states exist. The less compact one with $\Omega < \Omega_c$ has $L_o > 3L_s$ and is stable, being a minimum of the energy subject to the angular momentum being conserved (Counselman 1973, Hut 1980). The more compact one with $\Omega > \Omega_c$ has $L_o < 3L_s$ and is unstable; it may in any case be inaccessible if the orbit would be too small relative to the sizes of the bodies. The expressions for L_c and Ω_c are

$$L_c = 4I\Omega_c, \quad \Omega_c = (GM)^{1/2}\left(\frac{\mu}{3I}\right)^{3/4}, \tag{1}$$

where $M = M_1 + M_2$ is the total mass, $\mu = M_1M_2/M$ is the reduced mass, and $I = I_1 + I_2$ is the sum of the spin moments of inertia (assumed constant).

Many of the short-period extrasolar planetary systems for which tidal interactions are most important (having orbital periods less than about five days) have $L < L_c$ and therefore no tidal equilibrium; the orbit shrinks until the planet is destroyed. A few short-period systems with very massive planets are estimated to have $L > L_c$ (Levrard et al. 2009, Matsumura et al. 2010). In two of these, CoRoT-3 b and τ Boo b, the stellar spin appears to be approximately synchronized with the orbit (Husnoo et al. 2012), and these systems may already be in, or close to, a stable tidal equilibrium. In the case of τ Boo b (not mentioned by Levrard et al. or Matsumura et al.) it is likely that $L > L_c$ by only a narrow margin; the same is true of KELT-1 (Siverd et al. 2012) and CoRoT-15 (Bouchy et al. 2011), whose companions would usually be classified as brown dwarfs rather than planets. Some other short-period systems with $L > L_c$ could be evolving toward a stable equilibrium, although magnetic braking may eventually reduce L below L_c and destroy

the equilibrium. Many longer-period systems with massive planets also have $L > L_c$ but are not expected to undergo significant tidal evolution.

All satellite systems of solar-system planets have $L > L_c$. For the giant planets, $L \gg L_c$ and $L_o \ll 3L_s$; if a synchronously spinning satellite were placed in a circular orbit near the corotation radius (synchronous orbit) of a giant planet, it would migrate away from that radius and the planetary spin would not be greatly affected.

Tidal potential: the part of the gravitational potential due to body 2 that deforms body 1

Tidal dissipation generates heat in astrophysical bodies, which in some cases may be important for their structure and evolution. Apart from the well-known applications to the volcanic activity of Jupiter's moon Io and Saturn's moon Enceladus, this effect has been investigated mainly for short-period extrasolar planets undergoing tidal circularization, in an attempt to explain the unexpectedly large radii of many transiting planets (e.g., Bodenheimer et al. 2001, Ibgui & Burrows 2009). In fact, the orbital energy that must be dissipated to circularize a short-period planet can easily exceed the planet's internal binding energy, which suggests that rapid circularization, if possible, either makes the planet very bright or threatens to destroy it. Gu et al. (2003) identified a tidal inflation instability that may lead to the disruption of gas giants.

2. TIDAL DYNAMICS

2.1. Tidal Potential

Consider two bodies orbiting about their mutual center of mass. Let their masses be M_1 and M_2 and their centers of mass $\boldsymbol{R}_1(t)$ and $\boldsymbol{R}_2(t)$. Suppose that body 2 is a point mass or can be treated as such for the purposes of determining the motion and tidal deformation of body 2. When its gravitational potential $-GM_2/|\boldsymbol{r} - \boldsymbol{R}_2|$ is expanded in a Taylor series about $\boldsymbol{r} = \boldsymbol{R}_1$, we obtain

$$-\frac{GM_2}{|\boldsymbol{d}|}\left[1 + \frac{\boldsymbol{d}\cdot\boldsymbol{x}}{|\boldsymbol{d}|^2} + \frac{3(\boldsymbol{d}\cdot\boldsymbol{x})^2 - |\boldsymbol{d}|^2|\boldsymbol{x}|^2}{2|\boldsymbol{d}|^4} + \cdots\right] = -\frac{GM_2}{|\boldsymbol{d}|}\sum_{l=0}^{\infty}\frac{|\boldsymbol{x}|^l}{|\boldsymbol{d}|^l}P_l\left(\frac{\boldsymbol{d}\cdot\boldsymbol{x}}{|\boldsymbol{d}||\boldsymbol{x}|}\right), \qquad (2)$$

where $\boldsymbol{d} = \boldsymbol{R}_2 - \boldsymbol{R}_1$ is the orbital separation, $\boldsymbol{x} = \boldsymbol{r} - \boldsymbol{R}_1$ is the position vector with respect to the center of body 1, and P_l is the Legendre polynomial of degree l. The first term in this series is a uniform potential and has no effect, whereas the second term gives rise to a uniform acceleration, which causes the basic Keplerian orbital motion of body 1. The remaining part of the expansion defines the tidal potential Ψ, which gives rise to a nonuniform acceleration that deforms body 1. It can also be represented using solid spherical harmonic functions of the second degree and higher, i.e., $r^l Y_l^m(\theta, \phi)$ with $l \geq 2$ and $|m| \leq l$, where (r, θ, ϕ) are spherical polar coordinates with their origin at the center of body 1.

If body 1 is rotating, then for the purposes of computing the tidal deformation it is helpful to choose the axis of the coordinate system to coincide with the rotation axis. Let the orbit have semimajor axis a, eccentricity e, and inclination i with respect to the equatorial plane of body 1. In celestial mechanics i is known as the obliquity of body 1 (with respect to the orbit of bodies 1 and 2). The periodic variation of the separation vector due to the basic Keplerian orbital motion can be expressed through Fourier series, leading to an expansion of the complete tidal potential in a nonrotating frame in the form (cf. Kaula 1961, Polfliet & Smeyers 1990)

$$\Psi = \mathrm{Re}\sum_{l=2}^{\infty}\sum_{m=0}^{l}\sum_{n=-\infty}^{\infty}\frac{GM_2}{a}A_{l,m,n}(e,i)\left(\frac{r}{a}\right)^l Y_l^m(\theta,\phi)\mathrm{e}^{-in\Omega_o t}. \qquad (3)$$

Here $\Omega_o = (GM/a^3)^{1/2}$ is the mean orbital angular velocity, which we refer to as the orbital frequency (and is known as the mean motion in celestial mechanics). The dimensionless complex coefficients $A_{l,m,n}$ depend in a complicated way on e and i. The integers l and m are the degree

Table 1 Quadrupolar components of the tidal potential, correct to first order in eccentricity and obliquity

l	m	n	$\lvert A\rvert$	Description
2	0	0	$\sqrt{\frac{\pi}{5}}$	Static tide
2	2	2	$\sqrt{\frac{6\pi}{5}}$	Asynchronous tide
2	0	1	$3e\sqrt{\frac{\pi}{5}}$	Eccentricity tides
2	2	1	$\frac{1}{2}e\sqrt{\frac{6\pi}{5}}$	
2	2	3	$\frac{7}{2}e\sqrt{\frac{6\pi}{5}}$	
2	1	0	$i\sqrt{\frac{6\pi}{5}}$	Obliquity tides
2	1	2	$i\sqrt{\frac{6\pi}{5}}$	

and order of the spherical harmonic, respectively, and m is also referred to as the azimuthal wave number. The integer n labels temporal harmonics of the orbital motion.

In most applications the bodies are sufficiently well separated that the quadrupolar components ($l = 2$) are strongly dominant. In the special case of a circular, coplanar orbit ($e = i = 0$), the only terms present have $n = m$, and $l - m$ must be even. In the case of a circular, inclined orbit ($e = 0$), n is restricted to the range $[-l, l]$, and $l - n$ must be even (e.g., Ogilvie 2013). For the complete representation of an eccentric orbit, all values of n are required. However, if terms smaller than $O(e^p)$ can be neglected, then the largest value of $|n|$ that needs to be considered is $l + p$. **Table 1** gives the amplitudes, but not the phases, of the quadrupolar components of the tidal potential, correct to first order in e and i.

Because $Y_l^m(\theta, \phi) \propto \mathrm{e}^{\mathrm{i}m\phi}$, the phase of each tidal component is $\arg A_{l,m,n} + m\phi - n\Omega_\mathrm{o}t$. When $m \neq 0$, the phase rotates with angular velocity $n\Omega_\mathrm{o}/m$. The angular frequency of each component measured in a nonrotating frame is $\omega = n\Omega_\mathrm{o}$, which may be called the tidal frequency in the inertial frame. Of greater importance for the physical response of the fluid is the angular frequency measured in a frame that rotates with the spin angular velocity Ω_s (spin frequency) of body 1, $\hat{\omega} = n\Omega_\mathrm{o} - m\Omega_\mathrm{s}$, which may be called the tidal frequency in the fluid frame. When $m \neq 0$, the difference between ω and $\hat{\omega}$ is due to an angular Doppler shift. (In general, body 1 may rotate differentially, in which case $\hat{\omega}$ depends on position.)

The tidal frequencies in the fluid frame are therefore integer linear combinations of the spin and orbital frequencies; for the seven components listed in **Table 1**, these are plotted in **Figure 2**. As is discussed in Section 3, the Coriolis force plays a dominant role in the wave-like part of the tidal response when $|\hat{\omega}/\Omega_\mathrm{s}| < 2$ (and may still play an important role outside this interval), and it can be seen that all seven components typically have frequencies in this range, unless the body is far from the synchronous state.

As the eccentricity is increased from 0 toward 1, the time-dependence of the tidal forcing changes from a sinusoidal variation to one that is strongly peaked at the pericenter of the orbit. This is a result of the sensitivity of the tidal force to the orbital separation. The above expansion is still valid for large eccentricities, but a broad spectrum of frequencies is obtained (**Figure 3**). In a highly eccentric orbit, the tidal interaction has an impulsive character, consisting of a series of tidal encounters, each of which might be approximated as a parabolic orbit.

Tidal component: a single component of the tidal potential when it is decomposed into spherical harmonic functions and Fourier-analyzed in time

Inertial frame: a nonrotating frame of reference

Fluid frame: a frame of reference rotating with the spin angular velocity of body 1

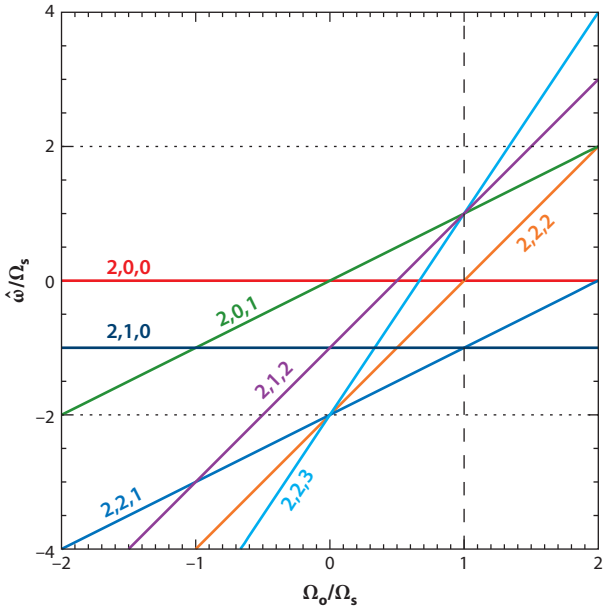

Figure 2

Tidal forcing frequencies for the seven lowest-order components listed in **Table 1**, labeled by l, m, n. The vertical axis is the ratio of the tidal frequency in the fluid frame to the spin frequency, whereas the horizontal axis is the ratio of the orbital frequency to the spin frequency. Each line has slope n and y-intercept $-m$. The dotted horizontal lines indicate the frequency range of inertial waves in a uniformly rotating body (see Section 3.5 below), whereas the dashed vertical line indicates the synchronous state.

2.2. Tidal Torque, Power, and Dissipation

If the tidal amplitude parameter ϵ is sufficiently small, the tidal response of a body can be determined using linear theory, as discussed in Section 3 below. In this approach, the tidal disturbance is treated as a small perturbation of a basic state, which is usually assumed to be steady and axisymmetric. To each component of the tidal potential there is an independent and linearly related response, which can be quantified using a response function. If a tidal potential component $\mathrm{Re}[\mathcal{A}(r/R)^l Y_l^m(\theta,\phi)\mathrm{e}^{-\mathrm{i}\omega t}]$ is applied to a body of nominal (e.g., mean or equatorial) radius R, and the resulting deformation of the body generates an external gravitational potential perturbation $\mathrm{Re}[\mathcal{B}(R/r)^{l+1} Y_l^m(\theta,\phi)\mathrm{e}^{-\mathrm{i}\omega t}]$ (possibly in addition to other components that are orthogonal to the applied one), then the complex dimensionless ratio $k_l^m(\omega) = \mathcal{B}/\mathcal{A}$ defines the potential Love number (named after A.E.H. Love). This is the most useful response function, because it is only through gravity that the tidal communication between the two bodies occurs. Of particular interest is the imaginary part $\mathrm{Im}[k_l^m(\omega)]$, which quantifies the part of the response that is out of phase with the tidal forcing and is associated with transfers of energy and angular momentum.

Potential Love number: a complex-valued, dimensionless, frequency-dependent response function relating the self-gravitational perturbation of a body to the applied tidal potential

Let the tidal power P and the tidal torque T be defined as the rates of transfer of energy and of the axial component of angular momentum from the orbit to the body (measured in the inertial frame, and averaged in time in the case of $m = 0$). It can be shown (e.g., Ogilvie 2013) that $P = \omega\mathcal{T}$ and $T = m\mathcal{T}$, where

$$\mathcal{T} = \frac{(2l+1)R|\mathcal{A}|^2}{8\pi G}\mathrm{Im}[k_l^m(\omega)]. \tag{4}$$

Tidal power: the rate of transfer of energy from the orbit to body 1

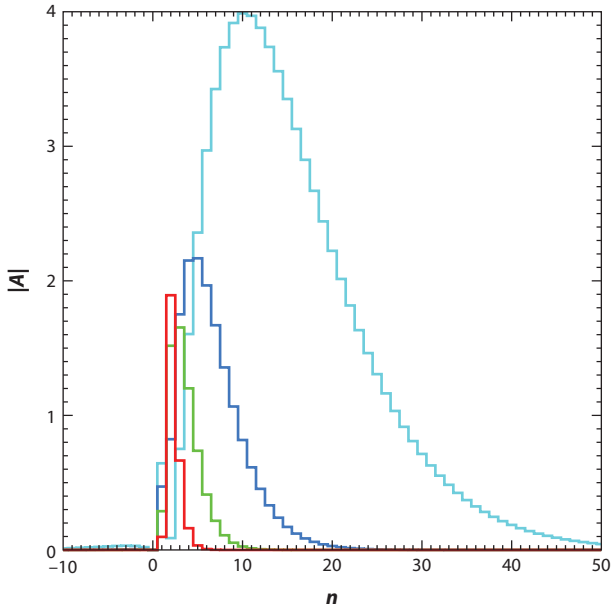

Figure 3

Amplitude $|A_{2,2,n}|$ of the $l = m = 2$ component of the tidal potential for obliquity $i = 0$ and eccentricities $e = 0.1$, 0.3, 0.5, and 0.7 (*red*, *green*, *blue*, and *cyan lines*, respectively).

In a frame that rotates with angular velocity Ω, the tidal torque is again T but the tidal power is $P - T\Omega$. When $m \neq 0$, the fact that $P = (\omega/m)T$ means that the tidal power vanishes in a rotating frame in which the tidal potential is stationary.

If the body rotates uniformly with angular velocity Ω_s, then the (frame-independent) tidal dissipation rate is $D = P - T\,\Omega_s = \hat{\omega}\mathcal{T}$. Although the torque, power, and dissipation rate are all quantities of second order in ϵ, they can be calculated within a linear analysis and are linearly proportional to the imaginary part of the response function. The difference between the dissipation rate and the power is the rate of change of the spin energy of the body, which vanishes in the fluid frame. Because D is a positive-definite quantity, we have the important result that $\mathrm{Im}[k_l^m(\omega)]$ has the same sign as $\hat{\omega}$. [A possible exception is that convection could in principle give energy to the tidal disturbance rather than dissipating it (Ogilvie & Lesur 2012).] $\mathrm{Im}[k_l^m(\omega)]$ should also vanish when $\hat{\omega} = 0$, because then the deformation is static in the fluid frame and should be in phase with the tidal forcing.

If the body rotates nonuniformly, then there is no simple global relation between D, P, and T. The dissipation rate cannot then be deduced from $\mathrm{Im}[k_l^m(\omega)]$ and ceases to be of such direct importance, except of course for tidal heating.

Several other parameterizations of the tidal response are in common use. Typically $\mathrm{Re}[k_l^m(\omega)]$ is a quantity of order unity, only weakly dependent on m and ω, and can be well approximated by its hydrostatic value. The evaluation of the hydrostatic Love number k_l (which is real and does not depend on m) for a spherical fluid body is a classical problem involving the equations of Clairaut and Radau (e.g., Kopal 1978); for a homogeneous body, $k_l = k_l^{\mathrm{hom}} = 3/[2(l-1)]$. [The apsidal motion constants long used in the theory of binary stars (e.g., Kopal 1978) are denoted by the same symbol k_l and are equivalent except that they are smaller by a factor of 2.] It is then common to write $|\mathrm{Im}[k_l^m(\omega)]|$ as k_l/Q, where Q is the tidal quality factor. It is also common to write k_l/Q as k_l^{hom}/Q', where Q' is a modified tidal quality factor; this has the advantage of combining Q with k_l, which

may not be known accurately as it depends on the interior structure, whereas $k_l^{\rm hom}$ has a simple analytical expression. [For giant planets, it is estimated that $0.1 < k_2 < 0.4$ (Gavrilov & Zharkov 1977, Kramm et al. 2012), although smaller values are possible for very centrally condensed models. For the Sun, $k_2 \approx 0.0351$, making it even more important to distinguish clearly between Q and Q'.] The phase lag in the tidal response is $1/Q$ and the time lag is $\tau = 1/(Q|\hat{\omega}|)$. To summarize, in the case of quadrupolar tides ($l = 2$) the various parameterizations of tidal dissipation are related by

Tidal quality factor (modified); phase lag; time lag: alternative parameterizations of the tidal response functions, not to be taken literally

$$\mathrm{Im}[k_2^m(\omega)] = \sigma \frac{3}{2Q'} = \sigma \frac{k_2}{Q} = k_2 \tau \hat{\omega}, \tag{5}$$

where $\sigma = \mathrm{sgn}\,\hat{\omega} = \pm 1$.

The expressions quality factor, phase lag, and time lag should not be taken literally. The above relations are based on a simplified conceptual model in which the tidal response resembles the hydrostatic one, but is slightly retarded in phase and unaffected in amplitude. However, if the tidal forcing resonates with a weakly damped normal mode of oscillation, especially if it is the fundamental mode as discussed in Section 3.1, it is possible in principle for $|\mathrm{Im}[k_l^m(\omega)]|$ to attain values much larger than unity because the amplitude of the tidal response greatly exceeds the hydrostatic one. No amount of phase lag could describe such a response. However, we can continue to use the above formal relations if we allow Q and Q' to be less than unity in such a situation (which is, however, unlikely to arise in practice).

Potential Love numbers can still be used to describe the tidal deformation of a body in a nonlinear regime, but then there can be interference between different components of the tide, and the Love numbers are no longer linear response functions of the body but depend on the amplitudes and relative phases of all applied tidal components.

It is particularly important to note that the tidal quality factor Q is not a fundamental material property of a body but is a dimensionless parameterization of a response function, which is partly why we favor the notation $\mathrm{Im}[k_l^m(\omega)]$. As well as depending on l, m, and ω, $\mathrm{Im}(k)$ depends on the internal structure and angular velocity of the body. In his first published paper, Goldreich (1963, pp. 258, 264) issues words of caution about this parameterization: "Q will in general vary with the frequency and amplitude of the tide and the size of the sphere in addition to its composition . . . In our discussions we shall use the language of linear tidal theory, but we must keep in mind that our numbers are really only parametric fits to a nonlinear problem."

2.3. Rate and Direction of Tidal Evolution

To lowest order in e and i, the rates of change of the orbital semimajor axis a, the spin angular velocity $\Omega_{\rm s}$ of body 1, the orbital eccentricity e, and the obliquity (spin-orbit misalignment) i of body 1 due to tidal dissipation in body 1 are given by

$$\frac{1}{a}\frac{\mathrm{d}a}{\mathrm{d}t} = -3\kappa_{2,2,2}\frac{M_2}{M_1}\left(\frac{R_1}{a}\right)^5 \Omega_{\rm o}, \tag{6}$$

$$\frac{1}{\Omega_{\rm s}}\frac{\mathrm{d}\Omega_{\rm s}}{\mathrm{d}t} = \frac{3}{2}\kappa_{2,2,2}\frac{L_{\rm o}}{L_{\rm s}}\frac{M_2}{M_1}\left(\frac{R_1}{a}\right)^5 \Omega_{\rm o}, \tag{7}$$

$$\frac{1}{e}\frac{\mathrm{d}e}{\mathrm{d}t} = \frac{3}{16}(4\kappa_{2,2,2} - 6\kappa_{2,0,1} + \kappa_{2,2,1} - 49\kappa_{2,2,3})\frac{M_2}{M_1}\left(\frac{R_1}{a}\right)^5 \Omega_{\rm o}, \tag{8}$$

$$\frac{1}{i}\frac{\mathrm{d}i}{\mathrm{d}t} = \frac{3}{4}\left[\kappa_{2,2,2}\left(1-\frac{L_\mathrm{o}}{L_\mathrm{s}}\right)+(\kappa_{2,1,0}-\kappa_{2,1,2})\left(1+\frac{L_\mathrm{o}}{L_\mathrm{s}}\right)\right]\frac{M_2}{M_1}\left(\frac{R_1}{a}\right)^5\Omega_\mathrm{o}, \tag{9}$$

where we introduce the notation

$$\kappa_{l,m,n} = \mathrm{Im}[k_l^m(n\Omega_\mathrm{o})] \tag{10}$$

for the imaginary part of the Love number corresponding to the tidal component labeled by l, m, and n, and

$$\frac{L_\mathrm{o}}{L_\mathrm{s}} = \frac{\mu[GMa(1-e^2)]^{1/2}}{I_1\Omega_\mathrm{s}} = \frac{GM_1M_2(1-e^2)^{1/2}}{I_1\Omega_\mathrm{s}\Omega_\mathrm{o}a} \tag{11}$$

is the ratio of the orbital angular momentum to the spin angular momentum of body 1 (if it has a fixed moment of inertia I_1). Note that these formulae are valid only for sufficiently small values of e and i. Our notation assumes that Ω_o and L_o are positive by definition, as are a, e, and i, whereas $L_\mathrm{s} = I_1\Omega_\mathrm{s}$ can be either positive or negative. The case $\Omega_\mathrm{s} < 0$ allows us to consider situations in which spin and orbit are (nearly) counter aligned. Results of this type can be found in the classic work by Darwin (1880), although expressed in a different notation; they are derived by considering the effects of the tidal torque and power on the spin and orbit. The effects of tidal dissipation in body 2 on the orbital semimajor axis and eccentricity, and on its spin angular velocity and obliquity, are simply obtained by interchanging the roles of the two bodies in this calculation.

Without considering yet the details of the tidal responses of astrophysical bodies, but assuming that $|\kappa| \lesssim 1$ (usually $\ll 1$) for each component, a number of observations can be made. First, tidal evolution occurs on a timescale that is much longer than the orbital timescale, if $\epsilon \ll 1$ as we have assumed. Second, tidal dissipation in the two bodies may be of comparable importance; the ratio of the factor $(M_2/M_1)(R_1/a)^5$ to the corresponding factor $(M_1/M_2)(R_2/a)^5$ when the roles are reversed can be expressed in terms of the mean densities of the bodies as $(\bar{\rho}_2/\bar{\rho}_1)^2(R_2/R_1)$, which suggests that dissipation in the smaller body can dominate the evolution of e (Goldreich 1963) and also of a before body 2 becomes synchronized. (Among exoplanetary systems, this ratio has values both less than and greater than unity.) Third, in systems for which $L_\mathrm{s} \ll L_\mathrm{o}$, spin evolution proceeds much more rapidly than orbital evolution.

If body 1 rotates uniformly with angular velocity Ω_s and the tidal dissipation rate is positive, then, as noted above, $\kappa_{l,m,n}$ must have the same sign as the sign of the tidal frequency in the fluid frame, $\hat{\omega} = n\Omega_\mathrm{o} - m\Omega_\mathrm{s}$, and must vanish when $\hat{\omega} = 0$. Note that $\kappa_{2,2,2}$ vanishes in the synchronous case $\Omega_\mathrm{s} = \Omega_\mathrm{o}$. Even in the lowest-order analysis presented here, numerous possibilities arise for the signs of the above rates of change. The signs of the contributions of the lowest-order tidal components to the rates of change of a, Ω_s, e, and i are summarized in **Figure 4**. In most cases there are competing contributions to $\mathrm{d}e/\mathrm{d}t$ and $\mathrm{d}i/\mathrm{d}t$, and the net result is not obvious (Jeffreys 1961, Goldreich 1963). The fourth contribution to $\mathrm{d}e/\mathrm{d}t$ comes with the largest weighting factor, but this might be offset by a weaker tidal response at the corresponding frequency.

In the unlikely event that all components have the same time lag τ, which is the case investigated in detail by Darwin (1880), Alexander (1973), Hut (1981), and many others, we have $\kappa_{l,m,n} = k_l\tau(n\Omega_\mathrm{o} - m\Omega_\mathrm{s})$ and obtain the simpler results,

$$\frac{1}{a}\frac{\mathrm{d}a}{\mathrm{d}t} = -6k_2\tau(\Omega_\mathrm{o}-\Omega_\mathrm{s})\frac{M_2}{M_1}\left(\frac{R_1}{a}\right)^5\Omega_\mathrm{o}, \tag{12}$$

$$\frac{1}{\Omega_\mathrm{s}}\frac{\mathrm{d}\Omega_\mathrm{s}}{\mathrm{d}t} = 3k_2\tau(\Omega_\mathrm{o}-\Omega_\mathrm{s})\frac{L_\mathrm{o}}{L_\mathrm{s}}\frac{M_2}{M_1}\left(\frac{R_1}{a}\right)^5\Omega_\mathrm{o}, \tag{13}$$

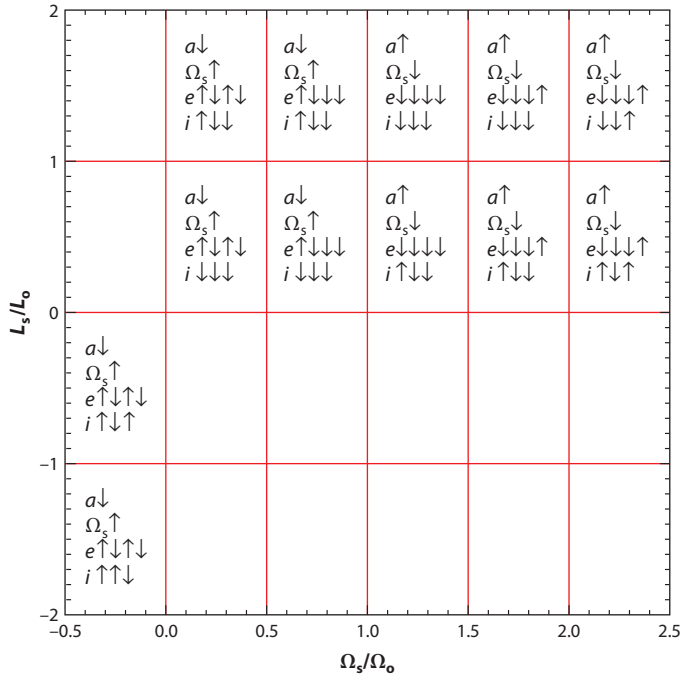

Figure 4

Signs of the contributions of the lowest-order tidal components to the rates of change of a, Ω_s, e, and i. The horizontal axis is the ratio of the spin frequency to the orbital frequency, whereas the vertical axis is the ratio of the spin angular momentum to the orbital angular momentum. Only the first and third quadrants are physically accessible. Upward and downward arrows indicate positive and negative rates of change, respectively. In the cases of e and i, the contributions are shown in the same order as that given in Equations 8 and 9. No further sign changes occur beyond the region plotted here.

$$\frac{1}{e}\frac{\mathrm{d}e}{\mathrm{d}t} = -\frac{3}{2}k_2\tau(18\Omega_\mathrm{o} - 11\Omega_\mathrm{s})\frac{M_2}{M_1}\left(\frac{R_1}{a}\right)^5\Omega_\mathrm{o}, \tag{14}$$

$$\frac{1}{i}\frac{\mathrm{d}i}{\mathrm{d}t} = -\frac{3}{2}k_2\tau\left[\Omega_\mathrm{s} + (2\Omega_\mathrm{o} - \Omega_\mathrm{s})\frac{L_\mathrm{o}}{L_\mathrm{s}}\right]\frac{M_2}{M_1}\left(\frac{R_1}{a}\right)^5\Omega_\mathrm{o}, \tag{15}$$

which would imply that the eccentricity is excited for $\Omega_\mathrm{s}/\Omega_\mathrm{o} > 18/11$ (Darwin 1880), whereas the obliquity is excited for $\Omega_\mathrm{s}/\Omega_\mathrm{o} > 2L_\mathrm{o}/(L_\mathrm{o} - L_\mathrm{s})$, if $0 < L_\mathrm{s} < L_\mathrm{o}$ (Hut 1981), or always, if $L_\mathrm{s} < 0$ (i.e., $\Omega_\mathrm{s} < 0$). The extension of these equations to arbitrary e and i under the assumption of a common time lag can be found in Leconte et al. (2010) and Matsumura et al. (2010) and was first derived by Alexander (1973).

3. LINEAR TIDES

3.1. Linear Response of a Star or Giant Planet to Harmonic Forcing

Let us consider in more detail the linear response of an astrophysical fluid body to periodic forcing by a single tidal component. A simple explicit example is provided by the highly idealized model of a homogeneous, incompressible, nonrotating, spherical fluid body with a viscosity proportional

f mode: a fundamental oscillation mode relying on the surface gravity of a body

to the pressure (cf. Sridhar & Tremaine 1992). Let the body have mass M, radius R, and dynamical frequency $\omega_{\rm d} = (GM/R^3)^{1/2}$, and let the dynamic viscosity be $\alpha p/\omega_{\rm d}$, where p is the pressure and α is a dimensionless viscosity coefficient. Then the linearized equations are solved by an irrotational displacement proportional to (but out of phase with) the tidal acceleration $-\nabla\Psi$, and the potential Love number can be shown to be

$$k_l^m(\omega) = \frac{3}{2(l-1)}\left[1 - \frac{\omega^2}{\omega_l^2} - \left(\frac{2l+1}{l}\right) {\rm i}\alpha\left(\frac{\omega}{\omega_d}\right)\right]^{-1}, \tag{16}$$

which is independent of m because of the spherical symmetry of the model. Here $\omega_l = [2l(l-1)/(2l+1)]^{1/2}\omega_{\rm d}$ is the natural frequency of the f mode of degree $l > 1$, which is the only oscillation mode that can be excited in this simple model. [This is the fundamental mode or surface gravity mode, first derived by Kelvin (Thomson 1863).] Note that the hydrostatic response $k_l = k_l^{\rm hom} = 3/[2(l-1)]$ is obtained in the low-frequency limit. The dynamics is exactly equivalent to that of a forced damped harmonic oscillator with natural frequency ω_l and damping coefficient $2(l-1)\alpha\omega_{\rm d}$. Now

$${\rm Im}[k_l^m(\omega)] = \frac{3(2l+1)}{2l(l-1)}\alpha\left(\frac{\omega}{\omega_{\rm d}}\right)\left[\left(1 - \frac{\omega^2}{\omega_l^2}\right)^2 + \left(\frac{2l+1}{l}\right)^2\alpha^2\left(\frac{\omega}{\omega_{\rm d}}\right)^2\right]^{-1}. \tag{17}$$

For a weakly damped oscillator ($\alpha \ll 1$) this response function has a strong peak close to the natural frequency (and attains $|{\rm Im}[k_l^m(\omega)]| \gg 1$, as mentioned in Section 2.2). Well below this frequency, the factor in square brackets is close to unity, corresponding to a frequency-dependent tidal quality factor given by $Q^{-1} \approx [(2l+1)/l]\alpha(\omega/\omega_{\rm d})$ or a frequency-independent tidal time lag $\tau \approx [(2l+1)/l](\alpha/\omega_{\rm d})$. (For this model, Q' and Q are equivalent because the body is homogeneous, and $\hat{\omega}$ and ω are equivalent because the body is nonrotating.) Note that even a damped simple harmonic oscillator has a frequency-dependent quality factor for forced oscillations. In the case of $l = 2$, the low-frequency response of the body is simply a hydrostatic spheroidal bulge with a small lag due to viscosity. If instead the body has a uniform kinematic viscosity ν, as in the model of Darwin (1880), then for $\omega \ll \omega_{\rm d}$ we have a similar result with α replaced by $(2l+1)(\nu/R^2\omega_{\rm d})$.

More realistic models of stars and planets support larger families of oscillation modes, allowing more opportunities for resonances with tidal forcing. (See also the sidebar, Tides in Black Holes.) Oscillation modes of the Sun and other stars have been studied in great detail for the purposes of helioseismology and asteroseismology (e.g., Aerts et al. 2010). Generally, this work either neglects rotation or treats it as a perturbation: The stellar or planetary model is spherically symmetric. Following Cowling (1941), the modes are classified as f modes (fundamental; i.e., surface gravity

TIDES IN BLACK HOLES

Tides can also be raised on black holes. Since the original work by Hartle (1973), a number of calculations of tidal torques on black holes have been carried out, making a variety of approximations that ensure that the tidal interaction is weak and of low frequency (e.g., Comeau & Poisson 2009). These are all consistent with the viewpoint that the horizon of the black hole behaves equivalently to a massive viscous shell with a viscous damping timescale comparable with its light-crossing time, as in the membrane paradigm (Thorne et al. 1986). The tidal torques that have been calculated then resemble equilibrium tides on such a shell, with an appropriate time lag (Poisson 2009). In reality, of course, energy and angular momentum are exchanged through gravitational waves crossing the event horizon. It may be expected that a richer response occurs when the tidal frequency is comparable with that of the quasi-normal modes of the black hole.

waves), p modes (pressure; i.e., acoustic waves), and g modes (gravity; i.e., internal gravity waves). The natural frequencies of f modes and p modes ($\gtrsim 10^{-4}$ Hz for the Sun) are generally too high ($\gtrsim \omega_d$) to be excited directly by tidal forcing, because the spin and orbital frequencies are usually small compared to the dynamical frequency of the body. The g modes, however, which propagate only in stably stratified (radiative) regions, form a dense spectrum at low frequencies and are good candidates for resonant excitation by tidal forcing. This is the basis of Zahn's theory of the dynamical tide (see Section 3.4 below).

As discussed in Section 2, tidal frequencies are often comparable to spin frequencies. This low-frequency part of the spectrum has received little attention in asteroseismology. The Coriolis force cannot be regarded as a small effect, and the wave equations are not separable in spherical harmonics. New types of oscillation mode (inertial waves) appear, which owe their existence to the Coriolis force. More interestingly, these low-frequency waves may not form classical normal modes and the tidal response may not be describable as a superposition of normal-mode resonances (see Section 3.5 below).

Internal waves supported by buoyancy and Coriolis forces play an important role in Earth's ocean and atmosphere, and have been widely studied through theory and experiment, but are less well known in astrophysics. They have properties quite different from acoustic or electromagnetic waves, being highly anisotropic and dispersive. In the fluid frame, the wave frequency depends only on the direction, and not on the magnitude, of the wave vector. Special directions are defined by gravity or rotation. Energy propagates at the group velocity, which is perpendicular to the wave vector and proportional to the wavelength. Internal waves are highly dispersive and do not steepen like acoustic waves, but when they exceed a critical amplitude they break, undergoing a local instability that causes their energy to be transferred to smaller scales and dissipated. In a closed domain, internal waves generally do not form normal modes with regular eigenfunctions, although the simplest cases are exceptions to this rule. The frequencies of internal waves are bounded and form a dense or continuous spectrum. The question then arises of how a rotating or stably stratified fluid responds to a tidal force with a frequency that lies within this spectrum.

p mode: an acoustic mode relying on compressibility

g mode: a global internal gravity mode relying on stable stratification

Internal gravity wave: an internal wave relying on buoyancy forces due to stable stratification

Dynamical tide: a tidal response that satisfies the time-dependent equations of fluid dynamics, and usually includes internal waves

Inertial wave: an internal wave relying on the Coriolis force due to rotation

Internal wave: a low-frequency, quasi-incompressible wave restored by buoyancy and/or Coriolis forces

Equilibrium tide: a hydrostatic approximation to the perturbations of density and pressure, accompanied by a displacement and velocity that may not be uniquely defined

3.2. Equilibrium and Dynamical Tides

The equilibrium tide is an approximation to the tidal response of a fluid body. It consists of a large-scale deformation of the body, which in the case of a quadrupolar tide ($l = 2$) is a spheroidal bulge. The density and pressure are distorted in order to achieve hydrostatic equilibrium in the instantaneous potential, which includes the distorted self-gravitational potential of the body in addition to the applied tidal potential. This hydrostatic balance is usually a good first approximation if the tidal frequency is small compared to the frequency of the f mode. In the model considered in Section 3.1, the equilibrium tide corresponds to the low-frequency limit $\omega \to 0$ of the tidal response.

A displacement of the fluid is required in order to bring about the tidal distortion. However, this is not uniquely defined in general and is a potential source of confusion or error, as discussed below. In any case, if the tidal frequency in the fluid frame is nonzero, the equilibrium tide does not satisfy the equation of motion exactly because the acceleration of the fluid is neglected in computing it, as is the effect of any damping forces. Corrections to the equilibrium tide generally include internal waves as well as nonwave-like components. Some or all of these corrections, or the complete tide calculated without a hydrostatic approximation, have been called the dynamical tide.

An unperturbed body in hydrostatic equilibrium satisfies

$$0 = -\frac{1}{\rho}\nabla p - \nabla\Phi, \tag{18}$$

where Φ is the self-gravitational potential of the body, but may also include the centrifugal potential corresponding to a uniform rotation (in which case the body is oblate). The curl of this equation implies that $\nabla\rho$ must be parallel to ∇p, which is also parallel to $\nabla\Phi$. Therefore ρ and p are functions of Φ only; we can also consider ρ to be a function of p only.

Let the body be perturbed by a tidal potential Ψ (satisfying $\nabla^2\Psi = 0$ inside the body) such that it maintains hydrostatic equilibrium. The linearized hydrostatic equation

$$0 = \frac{\rho'}{\rho^2}\nabla p - \frac{1}{\rho}\nabla p' - \nabla\Phi' - \nabla\Psi \tag{19}$$

is equivalent to

$$0 = -\nabla W + \left(\rho' - \frac{\mathrm{d}\rho}{\mathrm{d}p}p'\right)\frac{1}{\rho^2}\nabla p, \tag{20}$$

where $W = p'/\rho + \Phi' + \Psi$, and primes denote Eulerian perturbations. The curl of this equation implies that $\nabla(\rho' - \frac{\mathrm{d}\rho}{\mathrm{d}p}p')$ must be parallel to ∇p, as must ∇W. Therefore $\rho' - \frac{\mathrm{d}\rho}{\mathrm{d}p}p'$ must be a function of Φ only, and so must W. For an oscillatory tide (or tidal component) in which all perturbations have zero mean, they must in fact vanish. We deduce that

$$p' = -\rho(\Phi' + \Psi), \quad \rho' = -\frac{\mathrm{d}\rho}{\mathrm{d}p}\rho(\Phi' + \Psi). \tag{21}$$

The linearized Poisson equation then implies

$$\nabla^2\Phi' = -4\pi G\frac{\mathrm{d}\rho}{\mathrm{d}p}\rho(\Phi' + \Psi) \tag{22}$$

inside the body, whereas $\nabla^2\Phi' = 0$ outside. Given Ψ, this inhomogeneous Helmholtz-type equation (which can be related to the Clairaut and Radau equations if the unperturbed body is spherical) can be solved, subject to suitable conditions at the surface of the body, to determine Φ' and hence p' and ρ'. This is the equilibrium tide.

More problematic, though, is the tidal displacement $\boldsymbol{\xi}$ required to bring about these perturbations. Assuming adiabatic perturbations, we have

$$p' = -\gamma p\nabla\cdot\boldsymbol{\xi} - \boldsymbol{\xi}\cdot\nabla p, \quad \rho' = -\rho\nabla\cdot\boldsymbol{\xi} - \boldsymbol{\xi}\cdot\nabla\rho, \tag{23}$$

and so

$$0 = \rho' - \frac{\mathrm{d}\rho}{\mathrm{d}p}p' = -\left(\rho - \gamma p\frac{\mathrm{d}\rho}{\mathrm{d}p}\right)\nabla\cdot\boldsymbol{\xi}, \tag{24}$$

where $\gamma = (\partial\ln p/\partial\ln\rho)_s$ is the adiabatic exponent. If the body is stably stratified, having a nonzero (Brunt-Väisälä) buoyancy frequency N, then the quantity in brackets is nonzero, and we deduce that $\nabla\cdot\boldsymbol{\xi} = 0$: The displacement is incompressible. It then follows that

$$\boldsymbol{\xi}\cdot\boldsymbol{g} = \Phi' + \Psi, \tag{25}$$

where $\boldsymbol{g} = -\nabla\Phi = (\nabla p)/\rho$ is the (effective) gravitational acceleration. This relation determines the vertical displacement, and the horizontal displacement follows (nonlocally) from the condition $\nabla\cdot\boldsymbol{\xi} = 0$.

This solution is the standard equilibrium tidal displacement (Zahn 1966a, Goldreich & Nicholson 1989). It is the simplest form of displacement that achieves hydrostatic equilibrium in the distorted potential; under this volume-preserving motion, fluid elements retain their density and pressure and simply move them to a different location. However, if the body (or part of it) is adiabatically stratified (as in a convective zone, to a good approximation), then it is possible to add an arbitrary internal displacement satisfying the anelastic constraint $\nabla\cdot(\rho\boldsymbol{\xi}) = 0$ without changing ρ' or p'. Moreover, as discussed below, such an additional displacement is required in

order to satisfy the equation of motion in the low-frequency limit. The total displacement then satisfies neither $\nabla \cdot \boldsymbol{\xi} = 0$ nor $\nabla \cdot (\rho \boldsymbol{\xi}) = 0$, except in the case of a homogeneous body.

In an adiabatically stratified region, the linearized inviscid equation of motion for an arbitrary tidal frequency $\hat{\omega}$ in the fluid frame is exactly

$$-\mathrm{i}\hat{\omega}\boldsymbol{u} + 2\boldsymbol{\Omega}_\mathrm{s} \times \boldsymbol{u} = -\nabla W, \tag{26}$$

where $\boldsymbol{u} = -\mathrm{i}\hat{\omega}\boldsymbol{\xi}$ is the velocity perturbation. In the case of a nonrotating body, or in the limit $\hat{\omega}^2 \gg 4\Omega_\mathrm{s}^2$, this equation implies that $\nabla \times \boldsymbol{u} = 0$ and $\nabla \times \boldsymbol{\xi} = 0$: The tidal flow and displacement are irrotational (Goodman & Dickson 1998, Terquem et al. 1998). If we write $\boldsymbol{\xi} = \nabla U$, then the expression for ρ' implies that

$$\nabla \cdot (\rho \nabla U) = \frac{\mathrm{d}\rho}{\mathrm{d}p} \rho (\Phi' + \Psi). \tag{27}$$

This Poisson-type equation can be solved for U, subject to suitable boundary conditions, to determine $\boldsymbol{\xi}$.

However, in the limit $\hat{\omega}^2 \ll 4\Omega_\mathrm{s}^2$, Equation 26 implies that the tidal flow is in geostrophic balance and has a different form again. If $\hat{\omega}^2$ is comparable to $4\Omega_\mathrm{s}^2$, then the solution generally includes inertial waves (see Section 3.5 below).

To summarize, although the Eulerian perturbations of density and pressure are well defined in the hydrostatic limit $\hat{\omega}^2 \ll \omega_\mathrm{d}^2$, the form of the tidal displacement and velocity in the low-frequency limit depends significantly on the ordering of $\hat{\omega}^2$, N^2, and $4\Omega_\mathrm{s}^2$. (At sufficiently low tidal frequencies the assumption of adiabatic perturbations may also break down.) The standard equilibrium tidal displacement is obtained only in the limit $\hat{\omega}^2 \ll N^2$ and applies only in radiative zones.

3.3. Equilibrium Tides

As described above, a time-dependent equilibrium tide is associated with a large-scale velocity field. Any process that resists this flow leads to dissipation. Because the ordinary molecular viscosity is much too small to be of interest, the main candidate for providing linear damping of this flow is turbulent convection; nonlinear possibilities are discussed in Section 4.1 below. In the simplest approach, the effect of convection on the equilibrium tide is modeled as an effective viscosity, which can be estimated using an extension of the same mixing-length theory that is used to describe the convective heat flux in the theory of stellar structure.

It has long been recognized that the effective viscosity should be reduced by some factor when the tidal period is short compared with the typical convective timescale, as is often the case. (In the Sun, this timescale ranges from a month or longer near the base of the convective zone to a few minutes near the photosphere. In giant planets the convective timescale is generally longer because of the much smaller heat flux, although the applicability of mixing-length theory is uncertain because of the rapid rotation.) Different reduction factors were proposed by Zahn (1966b) and by Goldreich & Nicholson (1977) and Goldreich & Keeley (1977). Zahn's reduction factor is weaker, with $\nu \propto |\hat{\omega}|^{-1}$ and so $\mathrm{Im}(k) \propto Q'^{-1} \propto |\hat{\omega}|^0$ for large $|\hat{\omega}|$. Goldreich's reduction factor is stronger, with $\nu \propto |\hat{\omega}|^{-2}$ and so $\mathrm{Im}(k) \propto Q'^{-1} \propto |\hat{\omega}|^{-1}$ for large $|\hat{\omega}|$. Subsequent theoretical arguments (Goodman & Oh 1997, Ogilvie & Lesur 2012) favor this stronger reduction, which gives a frequency dependence similar to a Maxwellian viscoelastic model with a relaxation time related to the convective timescale.

Figure 5 illustrates the differences between these models in the case of the solar convective zone. The values of $\mathrm{Im}[k_2^m(\omega)]$ are found by calculating the total dissipation rate in the convective zone using the formulae quoted by Zahn (1989) and assuming that the velocity field is either

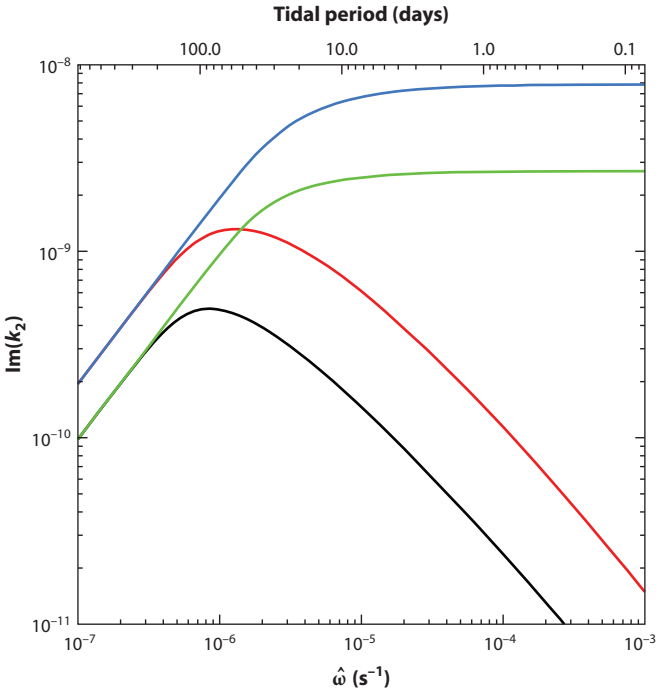

Figure 5

Frequency dependence of the dissipation of the nonwave-like tide in the convective region of a standard solar model. The turbulent viscosity is estimated using mixing-length theory, but is reduced using the prescriptions of Zahn (1966b) (*blue* and *green curves*) and Goldreich & Nicholson (1977) (*red* and *black curves*) in the forms quoted by Zahn (1989). The blue and red curves are computed assuming a standard equilibrium tide, whereas the green and black curves use the irrotational nonwave-like tide appropriate for a nonrotating convective region.

the standard equilibrium tide or the irrotational nonwave-like tide appropriate for a nonrotating convective region (discussed near Equation 27). For tidal periods of a few days or less, relevant for tidally interacting binary stars and extrasolar planets, the reduction factors can differ by more than one order of magnitude and the irrotational nonwave-like tide also leads to less dissipation. It must be emphasized that the results for other stars, or for the early Sun, could be very different.

In stars with deep convective envelopes, the scaling laws for the convective timescale t_c and for the effective viscosity ν and resulting tidal time lag τ, before any reduction factor is applied and omitting factors of order unity, are

$$t_c \sim \left(\frac{M_{\rm env}R^2}{L}\right)^{1/3}, \quad \nu \sim \left(\frac{LR^4}{M_{\rm env}}\right)^{1/3}, \quad \tau \sim \left(\frac{LM_{\rm env}^2R^7}{G^3M^6}\right)^{1/3}, \tag{28}$$

where $M_{\rm env}$ is the mass of the envelope, and M, R, and L are the stellar mass, radius, and luminosity, respectively. In a star that evolves to become a giant, τ can increase enormously, although this phase is relatively short-lived.

More recently, numerical simulations of turbulent convection have been used to address this issue. The results of Penev et al. (2007, 2009a,b) suggest that something closer to the prescription by Zahn (1966b) may be appropriate for intermediate frequencies, not for the reasons originally suggested but probably because the power spectrum of the convection in their simulations is less steep than the Kolmogorov spectrum assumed by Goldreich & Nicholson (1977). However, in

a more idealized model, Ogilvie & Lesur (2012) obtained results that favor the steeper reduction factor, and they even found that negative effective viscosities are possible, meaning that the convection can do work on the tidal disturbance. Further investigation is clearly required.

In giant planets the complex nature of the fluid may allow other forms of dissipation. Stevenson (1983) has argued that a large anomalous bulk viscosity can arise in a two-phase medium, such as that thought to occur in Saturn and possibly Jupiter, when the planet has cooled sufficiently that helium becomes immiscible with hydrogen and forms droplets. The action of this bulk viscosity on the tidal flow could provide an important amount of dissipation. (There is some uncertainty in Stevenson's analysis concerning the amount of compression involved in the tidal flow. Contrary to the argument presented above, he states that the tidal displacement is not nearly incompressible because the region of helium separation should be stably stratified.) The properties of the droplets, however, remain very uncertain. In the same paper, Stevenson mentions another possibility, which is that the equilibrium tide could induce dissipation as fluid cycles across a first-order phase transition at the interface between molecular and metallic hydrogen. However, current models indicate that a first-order phase transition, although possible in principle (McMahon et al. 2012), is not expected in Jupiter (French et al. 2012).

A controversial suggestion by Tassoul (1987), that tidal synchronization in close binary stars could proceed efficiently by means of Ekman pumping involving a viscous boundary layer, was refuted by Rieutord (1992) and Rieutord & Zahn (1997), but resurfaces occasionally in the literature. In fact, Tassoul's proposed mechanism cannot be described within the framework we have presented, or classified as linear or nonlinear, because it produces a torque that is of first order in the tidal amplitude parameter ϵ. This is unphysical and apparently relies on an artificial transfer of angular momentum across the surface of the star by a viscous torque, rather than by gravity. Internal viscous boundary layers could contribute to the dissipation of the equilibrium tide, however, in giant planets containing a solid core or other internal interfaces.

3.4. Dynamical Tides in Radiative Regions

Cowling (1941), who first analyzed the oscillation modes of a stably stratified (polytropic) stellar model, found that the $l = 2$ g modes form an infinite sequence with frequencies tending to zero. He noted that the tidal forcing in a binary star could resonate with the higher members of this sequence, but also suggested that nonlinear effects would limit the importance of such resonances.

Zahn (1970, 1975, 1977) considered the tidal forcing of low-frequency internal gravity waves in early-type stars, which have convective cores and radiative envelopes. Tidal dissipation occurs because of the radiative damping of the waves near the stellar surface, which is more effective for lower tidal frequencies (shorter radial wavelengths). For sufficiently low frequencies, the waves are strongly attenuated and do not reflect to form global g modes. In this regime the tidal response scales as $|\mathrm{Im}(k)| \propto |\hat{\omega}|^{8/3}$ and increases strongly with the size of the convective core. The dynamical tide is expected to be more important than the equilibrium tide for higher frequencies. The combined description of equilibrium and dynamical tides by Zahn (1977) has been very influential (Langer 2009).

A physical interpretation (Goldreich & Nicholson 1989) is that the waves are launched in a narrow region near the base of the radiative envelope, where the buoyancy frequency matches the tidal frequency and the radial wavelength is long enough to connect to the tidal forcing. They propagate to the surface where they are damped and deposit their angular momentum flux. For higher frequencies, partial reflection occurs near the surface, and the response function contains discrete resonant peaks. Savonije & Papaloizou (1983, 1984) made explicit numerical calculations, including nonadiabatic effects in full, for particular stellar models.

A similar treatment was applied to solar-type stars, which have a radiative core and a convective envelope, by Terquem et al. (1998) and Goodman & Dickson (1998). Internal gravity waves are launched near the outer boundary of the radiative core and propagate inward. Again, for sufficiently low frequencies, the waves are strongly attenuated by radiative damping and $|\mathrm{Im}(k)| \propto |\hat{\omega}|^{8/3}$; for higher frequencies, the response function contains discrete resonant peaks.

Recently, related calculations have been made for carbon-oxygen white dwarfs by Fuller & Lai (2012b). These stars are mostly radiative, but may contain narrow convective zones and/or sharp features in the profile of buoyancy frequency associated with abrupt changes in composition. Fuller & Lai find that the tidal response is approximately $|\mathrm{Im}(k)| \propto |\hat{\omega}|^5$, but modulated by peaks and troughs owing to interference effects involving a wave cavity. It appears that the waves are mainly excited in regions where the buoyancy frequency changes sharply, even if it remains above the tidal frequency.

Lubow et al. (1997) applied Zahn's dynamical tide to hot Jupiters, short-period extrasolar giant planets in which stellar irradiation makes the atmosphere stably stratified to a depth on the order of 100 bars. This is a promising mechanism for tidal dissipation in such planets that requires further investigation, as the analysis has many uncertainties related to rotation, winds, radiative damping, wave reflection, nonlinearity, etc. This problem would best be treated through numerical simulations that can treat simultaneously the nonlinear atmospheric dynamics and the tidally forced waves. [Earlier, Ioannou & Lindzen (1993) proposed that rotationally modified g modes could be excited by tidal forcing in Jupiter itself, but their model relies on the existence of a deep, weakly stable stratification, which is not generally accepted.]

The effects of uniform rotation on the dynamical tide in radiative regions have been examined for early-type stars by Savonije et al. (1995), Savonije & Papaloizou (1997), Papaloizou & Savonije (1997), and Witte & Savonije (1999a), and for solar-type stars by Savonije & Witte (2002) and Ogilvie & Lin (2007). In this work the centrifugal distortion of the star is neglected, being of second order in the ratio of the spin frequency to the dynamical frequency, but the Coriolis force is retained, either in full or in the so-called traditional approximation. This approximation [originally introduced by Laplace, and given its name by Eckart (1960)] retains only the part of the Coriolis force that acts on the horizontal motion, which may be assumed to be large compared to the vertical motion in a radiative zone if the tidal frequency is small compared to the buoyancy frequency.

Although each oscillation mode of a nonrotating star or planet is described by a pure spherical harmonic and can be driven linearly only by a tidal component of the same form, the Coriolis force in a rotating body breaks the spherical symmetry and couples spherical harmonics of different degrees l. Retention of the full Coriolis force, even in spherical geometry, requires two-dimensional computations, whereas the traditional approximation allows a convenient separation of variables that is analogous to, but more complicated than, the nonrotating case. The horizontal structure of the separated solutions is described by Hough modes, which are eigenfunctions of the Laplace tidal equations. Laplace (1775; see also Cartwright 1999, Deparis et al. 2013) originally derived these equations for a shallow, incompressible ocean of uniform depth on a rotating planet, and Hough (1897, 1898) studied their solutions in detail. Because each Hough mode contains multiple values of l, coupled by the Coriolis force, each tidal component can excite a richer variety of modes than in the nonrotating case.

Examples of frequency-dependent linear tidal responses of uniformly rotating stellar models are shown in **Figure 6** for 10 $M_\odot$ and in **Figure 7** for 1 $M_\odot$. In both cases the response is dominated by resonances with rotationally modified g modes at higher frequencies and with quasi-toroidal modes at lower frequencies. These latter modes owe their existence to the Coriolis force and are related to the r modes of Papaloizou & Pringle (1978) as well as the Rossby waves well known in geophysical fluid dynamics.

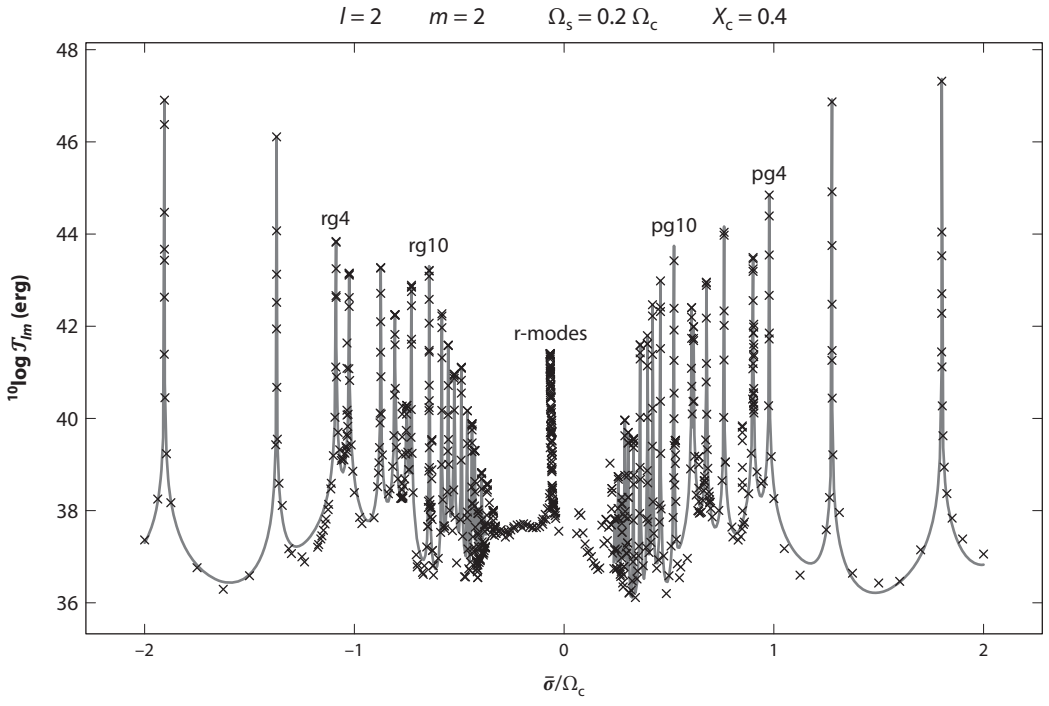

Figure 6

Linear response of a 10-$M_\odot$ star, uniformly rotating with $\Omega_s = 0.2\omega_d$, to $l = m = 2$ tidal forcing (reproduced, with permission, from Witte & Savonije 1999a). In our notation, the horizontal axis is $\hat{\omega}/\omega_d$. The quantity $|\mathcal{T}_{lm}| \approx 1.3 \times 10^{44}|\mathrm{Im}(k_2^2)|$ for this figure. Resonances with prograde and retrograde rotationally modified g modes of different radial orders are labeled. The low-frequency response involves quasi-toroidal modes.

Although the calculations of Savonije & Witte (2002) include the convective zone, the traditional approximation breaks down there and gives an inaccurate description of the inertial waves (Ogilvie & Lin 2004). Dynamical tides in convective zones are discussed in Section 3.5 below. The baseline value between resonances in **Figure 7** can perhaps be interpreted as being due to turbulent viscosity acting on the tide in the convective zone, although the role of the Coriolis force in this region under the traditional approximation is unclear. It corresponds to $|\mathrm{Im}(k_2^2)| \gtrsim 1 \times 10^{-7}$, which appears inconsistent with **Figure 5**, even under optimistic assumptions. It turns out that Savonije & Witte's implementation of mixing-length theory (and of the reduction factor) means that the turbulent viscosity is much larger than that estimated by Ogilvie & Lin (2007) and may also be much larger than the turbulent thermal diffusivity, contrary to expectations.

3.5. Dynamical Tides in Convective Regions

Models of stellar structure treat convective zones as being very slightly unstably stratified (i.e., superadiabatic), and interior models of giant planets are usually neutrally stratified (i.e., adiabatic). This is because, according to mixing-length theory, only a very small superadiabatic gradient is usually sufficient to provide the required heat flux through the body.

A simple approach to studying tides in convective regions is to neglect the convection per se and consider linear disturbances to a neutrally stratified basic state. If uniform rotation is also

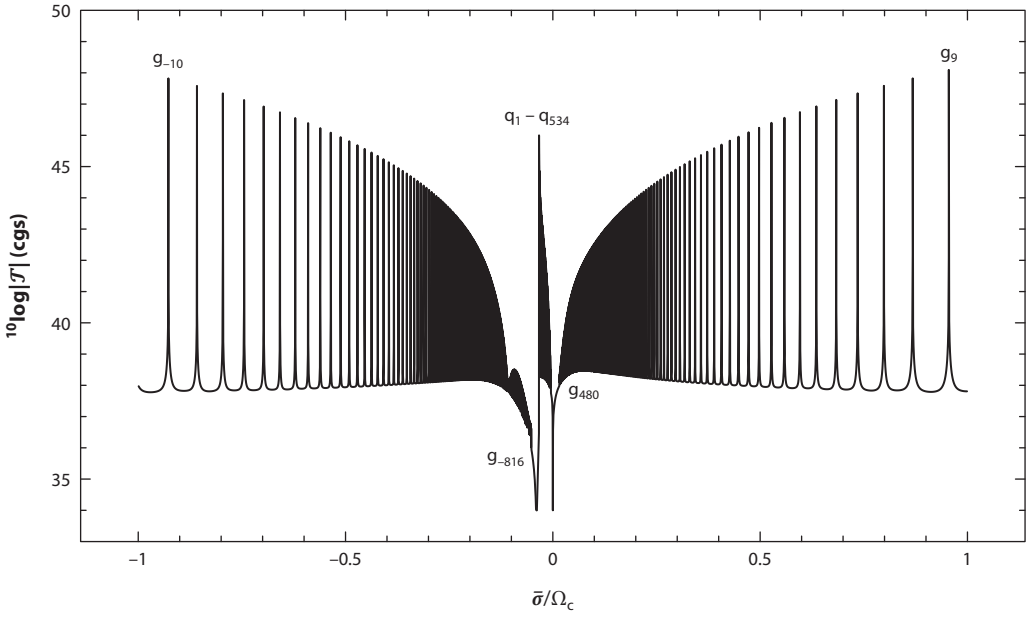

Figure 7

Linear response of a 1-$M_\odot$ star, uniformly rotating with $\Omega_s = 0.1\,\omega_d$, to $l = m = 2$ tidal forcing (reproduced, with permission, from Savonije & Witte 2002). In our notation, the horizontal axis is $\hat{\omega}/\omega_d$. The quantity $|\mathcal{T}| \approx 6.9 \times 10^{44}(R_\odot/R_1)|\mathrm{Im}(k_2^2)|$ for this figure. Resonances with prograde and retrograde rotationally modified g modes of different radial orders are labeled. The low-frequency response involves quasi-toroidal modes.

assumed for simplicity, then the low-frequency waves that comprise the dynamical tide are pure inertial waves restored by the Coriolis force (e.g., Greenspan 1968). If the body is fully convective, then the inertial waves propagate in a full sphere (or spheroid, more accurately). In other cases the waves may propagate only in a shell if they are excluded from either a solid planetary core or a stably stratified fluid core that the inertial waves cannot enter directly.

Linear inertial waves in a uniformly rotating, inviscid, incompressible fluid have been studied by Kelvin (Thomson 1880), Poincaré (1885), Bryan (1889), Cartan (1922), and many others (e.g., Greenspan 1968). They have remarkable mathematical properties. Their frequencies in the fluid frame satisfy $-2\Omega_s < \hat{\omega} < 2\Omega_s$, and the spatial structure of an inertial wave with a frequency in this range is governed by a second-order partial differential equation (named after Poincaré) that is hyperbolic; information propagates along characteristic surfaces that are inclined at an angle $\arcsin|\hat{\omega}/2\Omega_s|$ to the rotation axis. Waves with a given azimuthal wave number m satisfy an equation with similar properties in the meridional plane, with characteristic curves that are inclined at the same angle, which is also the inclination of the group velocity of the waves. Hyperbolic equations with conditions on the boundary of a closed domain generally give rise to ill-posed problems and the formation of singularities.

The global behavior of inertial waves in a reflective container is determined in part by the properties of the ray circuits, which depend sensitively on the angle of propagation and, therefore, on the wave frequency. In a full sphere or spheroid, the rays are space filling for most frequencies. It turns out that the waves can form smooth global normal modes at certain frequencies that are dense in the interval $(-2\Omega_s, 2\Omega_s)$. In a spherical shell, however, for most frequencies the rays are focused toward a small number of limit cycles known as wave attractors (Maas & Lam 1995,

Rieutord et al. 2001), which exist in certain bands of frequency, depending on the radius ratio of the shell. Generally speaking, inertial waves do not form smooth eigenmodes in a shell, although modes can be found localized around attractors when viscosity is introduced. In generalizations of this work, Dintrans et al. (1999) have found curved wave attractors for gravito-inertial waves in spherical geometry, as have Baruteau & Rieutord (2013) for inertial waves in a differentially rotating fluid.

In the past decade several studies have appeared examining linear dynamical tides in such configurations, showing that the Coriolis force gives rise to an enhanced tidal response in the frequency range $-2\Omega_s < \hat{\omega} < 2\Omega_s$, in which inertial waves can propagate and which is commonly found in applications (see **Figure 2**). Ogilvie & Lin (2004) considered a polytrope with a solid core and found that the tidal dissipation rate has a strong dependence on frequency in this range. This effect has been explored further by Ogilvie (2009) and Rieutord & Valdettaro (2010). The frequency dependence arises because of the sensitivity of the global propagation of inertial waves in a spherical shell to the inclination of the rays. It is more pronounced when the Ekman number $\mathrm{Ek} = \nu/2\Omega_s R^2$ is smaller and the rays can propagate further before dissipating. The behavior in the astrophysical limit of a very low Ekman number is complicated, although there seem to be intervals of frequency in which the dissipation rate becomes independent of or weakly dependent on the Ekman number. In a two-dimensional version of the same problem, it was shown that the dissipation rate is asymptotically independent of the magnitude and form of the small-scale dissipative mechanism (Ogilvie 2005); the wave attractor simply absorbs whatever energy flux is focused toward it. Although this result would be very appealing for astrophysical applications, its direct applicability is limited because of the competition between wave attractors and a singularity at the critical latitude, where the rays are tangent to the core (Goodman & Lackner 2009, Ogilvie 2009, Rieutord & Valdettaro 2010).

In contrast, studies of inertial waves in a full sphere, where the ray dynamics is much simpler, do not show this behavior. Instead, global normal modes, similar to those found by Bryan (1889), are excited, albeit rather weakly (Wu 2005a,b; Ivanov & Papaloizou 2010).

Examples of the frequency-dependent tidal responses are shown in **Figure 8** for an $n = 1$ polytrope with a perfectly rigid solid core, based on Ogilvie (2013). Responses are calculated for different values of the Ekman number in an effort to understand the astrophysical limit $\mathrm{Ek} \ll 1$; realistic values of Ek for giant planets are beyond current computational capabilities. For $|\hat{\omega}/\Omega_s| > 2$ the response is uninteresting and similar to an equilibrium tide, with $\mathrm{Im}(k) \propto \mathrm{Ek}$. A greatly enhanced, but strongly frequency-dependent, tidal response occurs for $|\hat{\omega}/\Omega_s| < 2$ because of the excitation of inertial waves. For a polytrope with a small core the response is dominated by near-resonances with two large-scale, global inertial modes of the full sphere, which are approximate solutions in the presence of a small core. When a larger core is introduced, normal modes are not excited and the response is dominated by wave singularities associated with the critical latitude on the inner boundary and with wave attractors (**Figure 9**; Ogilvie 2009).

A synthesis of these findings was attempted by Ogilvie (2013), who devised a method to obtain a frequency-averaged tidal response by means of an impulse calculation. The quantity computed is $\int \mathrm{Im}(k_l^m)\mathrm{d}\hat{\omega}/\hat{\omega}$, integrated over the low-frequency part of the spectrum where inertial waves are found. It can be taken as a gross measure of the tidal response in this range of frequencies, when the details of the response curve are washed out. In particular, for the $l = m = 2$ tidal component most often considered, the analytical result for a uniformly rotating homogeneous fluid body with a perfectly rigid core of fractional size f is

$$\int \mathrm{Im}(k_2^2)\frac{\mathrm{d}\hat{\omega}}{\hat{\omega}} = \frac{100\pi}{63}\left(\frac{\Omega_s}{\omega_d}\right)^2 \frac{f^5}{1-f^5}. \tag{29}$$

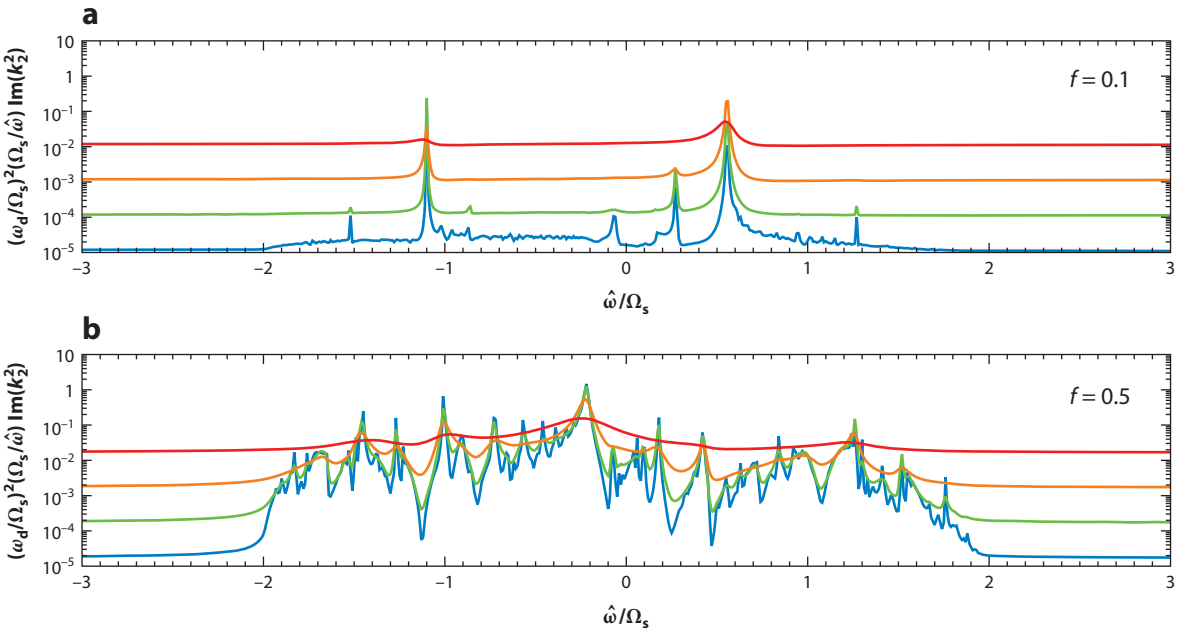

Figure 8

Linear response of a uniformly (and slowly) rotating $n = 1$ polytrope, with a perfectly rigid solid core of fractional size (*a*) $f = 0.1$ or (*b*) $f = 0.5$, to $l = m = 2$ tidal forcing, as in Ogilvie (2013). The fluid is viscous and the Ekman number is $\mathrm{Ek} = 10^{-3}$ (*red line*), 10^{-4} (*orange line*), 10^{-5} (*green line*), or 10^{-6} (*blue line*).

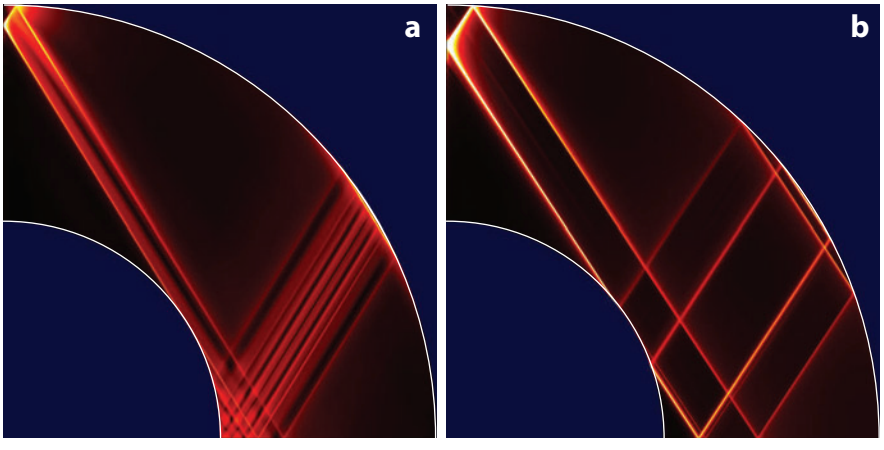

Figure 9

Structure of the velocity perturbation $|\boldsymbol{u}|$ in a meridional quarter-plane for the $l = m = 2$ tide forced in a uniformly (and slowly) rotating homogeneous fluid body with a perfectly rigid solid core of fractional size $f = 0.5$, as in Ogilvie (2009). The fluid experiences a frictional damping force with a damping coefficient $\gamma = 10^{-3}\,\Omega_s$. In the case of (*a*) $\hat{\omega}/\Omega_s = 1.05$ the response is dominated by a beam of inertial waves emitted from the critical latitude on the inner boundary. In the case of (*b*) $\hat{\omega}/\Omega_s = 1.10$ it is dominated by an inertial wave attractor.

Several points are noteworthy. First, the result is independent of the viscosity, which is consistent with the fact that the response curve involves more features, with higher peaks and lower troughs, as the viscosity is reduced. Second, the tidal response of inertial waves increases with the square of the spin frequency, which is an important general property (valid for $\Omega_s \ll \omega_d$; tidal dissipation in a rapidly rotating body has not yet been calculated). Third, the response vanishes for a full sphere and increases strongly with the core size, even diverging in the limit of a thin shell, although it should be noted that the core is assumed to be perfectly rigid and the planet to be of uniform density. (Tides in shallow rotating fluid layers, first considered by Laplace, are worthy of further investigation.)

It turns out that the dependence f^{2l+1} for $f \ll 1$ occurs for all sectoral harmonics ($m = l$), whereas for tesseral harmonics ($m \neq l$) the frequency-integrated response remains nonzero as $f \to 0$. This difference in behavior occurs because tesseral harmonics are able to resonate with the global inertial modes of a homogeneous full sphere, whereas the sectoral harmonics are not. Care is required, though, because the $l = 2$ tesseral harmonics have only formal resonances with the spin-up and spin-over modes, which involve rigid rotations and have no associated dissipation, and these dominate the integrated responses.

When the body is inhomogeneous, global modes can be excited even by sectoral harmonics in a full sphere. The strong dependence of the frequency-averaged response on the core size is not seen in polytropes of higher index that resemble centrally condensed stars. If the solid core is replaced by a fluid core such that the density is discontinuous at the interface between fluid layers, then behavior is found that is qualitatively similar but generally weaker, especially if the discontinuity is small. This occurs because of the different responses of the layers and because the inertial waves undergo partial internal reflection at the interface.

To summarize, as the size of the core is increased, a transition occurs from a response involving classical resonances with global normal modes to a richer one in which wave singularities are dominant. Generally a greater tidal response in inertial waves is obtained by having a larger core or a greater density contrast. It is expected that differential rotation will also increase the richness of the response (Ogilvie & Lin 2004, Baruteau & Rieutord 2013).

3.6. Tidal Encounters

Press & Teukolsky (1977) performed a classic calculation of the energy deposited in the oscillation modes of a nonrotating star during a parabolic tidal encounter. Although their study was motivated by the binary capture mechanism of Fabian et al. (1975), it is also relevant to the process by which extrasolar planets can reach short-period orbits through tidal interaction with the star if they start from a highly elliptical orbit. [Errors in the numerical results of Press & Teukolsky (1977) were corrected by Giersz (1986), Lee & Ostriker (1986), and McMillan et al. (1987).] An important dimensionless parameter in the problem is, in our notation,

$$\eta = \frac{\omega_d}{\Omega_{max}} = \left(\frac{M_1}{M}\right)^{1/2} \left(\frac{d_{min}}{R_1}\right)^{3/2}, \tag{30}$$

where $\Omega_{max} = (GM/d_{min}^3)^{1/2}$ is the circular orbital angular velocity at the minimum orbital separation, d_{min}. The parameter η is a measure of the duration of periastron passage, relative to the dynamical timescale of the star, and is not directly related to the tidal amplitude parameter ϵ. It is expected that $\eta \gtrsim 1$ in order to avoid tidal disruption; in the case of an incompressible fluid body with $M_1 \ll M$, tidal disruption occurs for $\eta \lesssim 2.2$ (Kosovichev & Novikov 1992, Sridhar & Tremaine 1992). In a neutrally stratified star, the energy transferred, ΔE, is found to decline exponentially with η for large η; this is because the orbital motion at pericenter is too

slow to excite the f mode and p modes of the star efficiently. In a stably stratified star, however, ΔE declines as an inverse power of η, because of the excitation of low-frequency g modes.

Lai (1997) has extended these calculations to include uniform rotation within the traditional approximation, whereas Papaloizou & Ivanov (2005) and Ivanov & Papaloizou (2007) have included the full Coriolis force in the case of a coreless model with neutral stratification. Here, global inertial modes dominate the response for large η, and the transfers of energy and angular momentum in the tidal encounter, ΔE and ΔJ, depend on the rotation rate through the parameter Ω_s/Ω_{max}, as well as on η. Papaloizou & Ivanov (2010) were able to include a solid core, even though global inertial modes do not occur, by solving an initial-value problem for linear tidal disturbances in a parabolic encounter. They found that ΔE increases with the size of the core, which is broadly in line with the findings described in Section 3.5 for periodic tides.

Indeed, a synthesis of the results on periodic and aperiodic tides can be achieved through the frequency-dependent response function $k_l^m(\omega)$. The energy and angular momentum transferred in a parabolic encounter are equal to integrals of $\mathrm{Im}[k_l^m(\omega)]$ over all frequencies, with two different weightings involving the temporal Fourier transform of the tidal potential for a parabolic orbit. This produces a viscosity-independent result that integrates out all the complicated structure in the response curve.

This calculation of ΔE and ΔJ, which implicitly assumes that the body is unperturbed before the encounter, is strictly relevant for a highly eccentric orbit only if the tidal disturbance is efficiently damped within an orbital period. If there is interference between waves excited by successive encounters, then the coupled dynamics of the orbit and oscillation modes can be initially chaotic (Mardling 1995a), although it becomes regular under the action of dissipation (Mardling 1995b).

3.7. Discussion of Linear Theory

We have described several situations in which linear theory predicts a tidal response whereby $\mathrm{Im}(k)$ varies strongly as a function of $\hat{\omega}$, often with peak and trough values that differ by several orders of magnitude. It should be borne in mind that these response functions are based on linear theory with various idealizations concerning the basic state. (Even so, they are computationally demanding because of the need for very high resolution in the spatial and frequency domains.) They also assume a steady-state response; the peak values, or tidal resonances, require multiple wave reflections and tidal periods to become established.

Nevertheless, it is important to ask how an astrophysical system evolves in such cases. The tidal frequency in the fluid frame for a particular tidal component, $\hat{\omega} = n\Omega_o - m\Omega_s$, is an integer linear combination of the spin and orbital frequencies, both of which evolve as a consequence of tidal dissipation (except in the case of $m = 0$). The evolution of $\hat{\omega}$ is most rapid at the peaks of the response curve, and the system therefore spends most of its time evolving slowly through the troughs. This suggests that strong tidal resonances are short-lived and of little importance.

However, Witte & Savonije (1999b, 2001) have found that systems can sometimes lock into tidal resonances and undergo relatively rapid evolution. In general, evolution through the troughs of the response curve of one tidal component may be accelerated or reversed by the effects of other tidal components, or by magnetic braking or stellar evolution, which can change the shape of the response curve and the locations of peaks and troughs. If these other effects cause an evolution toward a tidal resonance that itself causes an evolution in the opposite direction, then a balance can be attained in which the resonance is entered into to a certain degree. Strong resonant locking is most likely to happen when there is a near cancellation between the rates of change of $n\Omega_o$ and of $m\Omega_s$; for binary stars, in which the spin moment of inertia is small compared with the orbital

moment of inertia, this condition can be met for a component with a large value of n, which may have appreciable amplitude if the eccentricity is not small.

It should be borne in mind that models of stellar and planetary interiors have been developed, for the most part, in order to understand their gross properties and long-term evolution, not for a detailed study of their dynamical perturbations. In fact, stellar interior models are increasingly being used for seismology, but this mostly involves acoustic waves. There are numerous uncertainties concerning the behavior of low-frequency waves in stellar and planetary interiors. In particular, it is not clear how to model correctly the behavior of inertial waves in a convective medium. In models of the Sun, for example, $-N^2$ is positive in the convective zone and rises upward, exceeding $4\Omega_s^2$ above about $0.9\,R_\odot$. Should the linearized equations include this unstable stratification, which would significantly alter the properties of the waves? Or is the unstable stratification effectively neutralized by the existence of the convection? Does convection damp the waves like a viscosity or scatter or affect them in some other way? What are the effects of magnetic fields, differential rotation, and imperfect reflections of the waves from the boundaries of the convective region?

4. NONLINEAR TIDES

4.1. Nonlinear Equilibrium Tides

As described in Section 3.3, the equilibrium tide consists of a spheroidal bulge that is usually time dependent in the fluid frame and is then associated with a large-scale velocity field. In Section 3.3, we considered linear damping mechanisms, such as the interaction of the tidal flow with turbulent convection, which lead to a dissipation rate proportional to ϵ^2, where ϵ is the tidal amplitude parameter. It is also possible that the flow could be damped as a result of its intrinsic instability. It would be natural for such a mechanism to set in, or to dominate, above a critical tidal amplitude and to lead to a dissipation rate that is no longer proportional to ϵ^2. This would mean that $|\mathrm{Im}(k)|$ depends on ϵ, although it is then not a linear response function but a parameterization of a nonlinear response (Goldreich 1963).

Press et al. (1975) noted that the Reynolds numbers of tidal flows in close binary stars are very large. They proposed that this leads to turbulence and to a turbulent viscosity ν_t, such that the effective Reynolds number of the tidal flow based on ν_t is a modest value of order unity, Re_t. The resulting scaling relations are $\nu_t \sim \mathrm{Re}_t^{-1}\epsilon R^2|\hat{\omega}|$ and $|\mathrm{Im}(k)| \sim \mathrm{Re}_t^{-1}\epsilon(\hat{\omega}/\omega_d)^2$. However, it remains to be demonstrated whether this mechanism works in the presence of either pre-existing turbulence (in convective zones) or stable stratification (in radiative zones).

A more sophisticated viewpoint is that the instability would take the form of a resonant coupling of the internal wave modes of a rotating and/or stably stratified body. This takes into account the fact that the tidal flow has a well-defined oscillation frequency and spatial structure. If two internal modes can be found with frequencies and spatial structures that are linked by those of the tidal flow, then that pair of modes may be destabilized. The density of the spectrum of internal waves makes such a coincidence more probable. A perfectly tuned pair of undamped modes grows at a rate proportional to ϵ, but this parametric instability may be reduced or suppressed by damping or detuning of the modes. It is much more difficult to determine the nonlinear outcome of such instabilities and the resulting dissipation rate, because a multitude of interacting internal waves may be involved.

An important example is the elliptical instability, which is a parametric resonance of internal (usually inertial) waves due to an elliptical deformation of the streamlines of a rotating flow

(Kerswell 2002). This is precisely the situation when a spheroidal tidal bulge is generated in a rotating body. Elliptical instability has been investigated by means of laboratory experiments, linear analysis, and numerical simulations, mainly for flows without stable stratification, in which pairs of inertial waves are destabilized through their coupling to the deformation. Its application to astrophysical systems, where it has sometimes been called tidal instability, has been discussed by Rieutord (2004), Le Bars et al. (2010), and Cébron et al. (2010, 2013). A necessary condition for elliptical instability involving a pair of inertial waves in a uniformly rotating body is that the primary tidal flow has $|\hat{\omega}| < 4\Omega_s$ (so that it can couple to two secondary inertial waves, each having $|\hat{\omega}| < 2\Omega_s$). For the $l = m = n = 2$ tide with $\hat{\omega} = 2(\Omega_o - \Omega_s)$ this condition is $-1 < \Omega_o/\Omega_s < 3$, which is a wider range than that for tidal forcing to excite inertial waves directly. Even so, the instability would not be allowed in the majority of stars hosting hot Jupiters, where $\Omega_o/\Omega_s > 3$.

In order to observe the elliptical instability in experiments or simulations, where the Ekman number $\mathrm{Ek} = \nu/2\Omega R^2$ is much larger than in astrophysical bodies, the tidal amplitude must also be made much larger than is usually realistic. This situation favors the dominance of large-scale modes in the nonlinear outcome of the instability. Although attempts have been made to deduce scaling relations, and it is claimed that an order-unity change in the basic flow is commonly obtained, it is not yet clear what the nonlinear outcome would be for realistic values of Ek and ϵ.

A limitation of much of this work is that it focuses on the case in which the deformation is stationary in the inertial frame. This means that the elliptical instability takes the special form of the spin-over mode, which has the same property. A typical nonlinear outcome is a steady or recurrent tilting of the spin axis of the body, and this has been proposed as an explanation of the spin-orbit misalignments observed in exoplanetary systems (see Section 5.3 below). However, a simple tilting of the stellar spin axis is not a permissible outcome; in order to conserve the total angular momentum of the system, the orbital angular momentum would have to increase in magnitude, requiring an increase in the total energy of the system, whereas in fact the total energy can only decrease as a result of dissipation.

In an astrophysical system, where the tidal potential and deformation rotate at the orbital frequency and the values of Ek and ϵ are much smaller, it appears more likely that the elliptical instability, if present, generates turbulence through the excitation of smaller-scale waves. In a local computational model, the instability either saturates through the formation of long-lived columnar vortices (Barker & Lithwick 2013a) or generates three-dimensional turbulence, in the presence of a magnetic field (Barker & Lithwick 2013b).

Another interesting line of research has investigated nonlinear couplings of tides and global oscillation modes (f, p, and g) of nonrotating stellar models (Kumar & Goodman 1996; Weinberg et al. 2012, 2013). It provides a weakly nonlinear theory that includes quadratic terms that couple different modes. A conventional application of this work is that, in radiative zones, the equilibrium tide can excite pairs of g modes by parametric resonance and may thence find a route to dissipation. Kumar & Goodman (1996) showed that this mechanism could be effective in damping the f mode excited in a tidal encounter. For a solar-type binary with a moderately eccentric orbit, Weinberg et al. (2012) find that parametric instability of the equilibrium tide occurs only for orbital periods less than about one day, because the unstable modes are concentrated near the core of the star and connect very weakly with the equilibrium tide. Using the same formalism, Weinberg et al. (2013) find a quite different, nonresonant instability of a p–g mode pair, even for a static (time-independent) equilibrium tide. This result has been challenged (Venumadhav et al. 2013) and appears to violate the energy principle; it may indicate the inconsistencies of using truncated expansions. As yet, this approach has not included the important effects of rotation. The assumption of a mode expansion may be problematic if the waves do not form global modes in the linear regime or if the waves are of sufficient amplitude to break.

4.2. Nonlinear Dynamical Tides

In Sections 3.4 and 3.5 we discussed the tidal excitation of internal waves and their dissipation through linear damping mechanisms. Both gravity waves and inertial waves may be dissipated more effectively through nonlinear processes. Internal waves break if they exceed a critical amplitude, which is approximately when the displacement in the direction parallel to gravity (or perpendicular to the rotation axis, in the case of inertial waves) is equal to the wavelength in that direction divided by 2π. Under these conditions, the wave so distorts the background stratification or vorticity that a localized convective or shear instability occurs, and turbulence may be generated. Below the breaking amplitude, internal waves may still be unstable through mode couplings and may transfer their energy to other waves, usually of smaller scale. In an unbounded medium or periodic box, in the absence of dissipative effects, a plane internal wave of any amplitude is unstable in this way (Mied 1976).

Goodman & Dickson (1998) noted that the dynamical tide in a star similar to the present Sun, forced by a binary companion in an eccentric orbit, can easily exceed the breaking amplitude in the innermost wavelengths near the stellar center and is then bound to be significantly damped. In fact, the level of nonlinearity in the wave increases strongly toward the center because of the concentration of the wave energy into a small volume. Ogilvie & Lin (2007) applied a similar idea to the host stars of hot Jupiters, where the stellar rotation is slow compared to the orbit and the eccentricity is negligible; they found that, for a model based on the present Sun, a companion of more than about three Jupiter masses would generate waves that could break near the center, but also noted that the threshold depends on the stellar model. More detailed calculations were made by Barker & Ogilvie (2010), who also performed numerical simulations of the breaking process. Among solar-type stars, the threshold companion mass decreases with increasing stellar mass and with increasing age. Older or more massive stars have a steeper stratification near the center because of their chemical evolution.

Numerical simulations of internal gravity waves approaching the stellar center (Barker & Ogilvie 2010, Barker 2011) show that, if the breaking amplitude is exceeded, the waves are almost completely dissipated. Angular momentum is deposited, and an expanding core is formed in which material is spun up to the orbital frequency. Waves approaching the boundary of this core encounter a critical layer (at which the angular velocity of the fluid matches that of the wave) that causes them to be dissipated there. The planet donates its orbital angular momentum to the stellar core. The resulting dissipation is equivalent to $Q' \approx 1.5 \times 10^5 \ (P/\mathrm{day})^{8/3}$ for the Sun, where P is the orbital period; this estimate varies by no more than a factor of five for solar-type stars between 0.5 and 1.1 $M_\odot$. This mechanism should lead to the destruction of sufficiently massive hot Jupiters with orbital periods of about one day within a few million years of the commencement of wave breaking. (However, if the companion is sufficiently massive, then a tidal equilibrium may be approached instead, because the star can be spun up to match the increasing orbital frequency; see Section 5.3 below.)

In fact, this process is similar to one described by Goldreich & Nicholson (1989) in which early-type stars with close binary companions become synchronized from the outside in, as internal gravity waves generated by tidal forcing near the base of the radiative envelope are absorbed by a critical layer that advances inward from the stellar surface. This can be seen as a nonlinear modification of Zahn's dynamical tide, which is more effective in damping the waves and producing robust dissipation.

In principle, the process of an advancing critical layer could be initiated below the breaking amplitude as waves deposit angular momentum gradually by linear radiative damping near the stellar center (or surface). However, various processes may prevent the formation of the required

differential rotation, such as hydrodynamic instability or magnetic coupling. It is not clear how this mechanism applies to eccentricity tides, where there are multiple tidal components with different angular pattern speeds (**Table 1**).

Linear theories of dynamical tides often exhibit strong resonant peaks in the tidal response at the frequencies of global internal modes, where tidally forced waves reflect and interfere constructively (Section 3.4). If such a resonance occurs, the waves are much more likely to break, in which case the torque is reduced to a nonresonant value. The passage through such a tidal resonance could therefore initiate an advancing critical layer. Models that rely on locking into a linear resonance may be compromised by the breaking of the waves. This was acknowledged by Witte & Savonije (1999b), but appears not to have been estimated accurately; Witte & Savonije (2002) capped their resonant torques by limiting the velocity perturbation to the sound speed at the stellar center, but in fact the relevant comparison is to the much smaller wave speed of internal (gravity) waves.

Nonlinear processes have also been discussed for inertial waves in convective regions. Goodman & Lackner (2009) argued that a fraction of the inertial wave flux generated at the critical latitude on the inner boundary of a spherical shell would be subject to dissipation through wave breaking. By preventing multiple reflections within the shell, this process would strongly reduce the frequency dependence of the tidal response. Jouve & Ogilvie (2014) have simulated an inertial wave attractor in linear and nonlinear regimes; as waves are focused toward the attractor, they may exceed the breaking amplitude and produce waves of smaller scale before they themselves can reach the scale of viscous dissipation, but the total dissipation rate is not greatly reduced compared with the linear theory. Favier et al. (2014) have performed numerical simulations of forced inertial waves in spherical shells. The results for low amplitudes agree with the linear theory, and for higher amplitudes the dominant nonlinear effect they find is the development of zonal flows, in which the angular velocity depends on cylindrical radius in a complicated way that is related to the locations at which the inertial waves are preferentially dissipated. As these zonal flows build up, they increasingly alter the propagation and dissipation of the inertial waves. This interaction of waves and a mean flow may be self-regulating, although in some cases hydrodynamic instability is seen to occur.

An important nonlinear aspect of tidal interactions, therefore, is the development of differential rotation through the nonuniform deposition of angular momentum by tidal disturbances, and the interaction of this differential rotation with the tides. This adds another layer of complexity to the problem, which is only just beginning to be explored in detail.

5. APPLICATIONS TO OBSERVED SYSTEMS

5.1. Direct Observations of Tides in Stars

Direct observations of tides in stars and giant planets are limited, even within the Solar System. For decades, though, ellipsoidal variations in the light curves of close binary stars have been understood as being due to the changing aspect of tidally deformed stars (e.g., Kopal 1978). Recently, Welsh et al. (2010) used *Kepler* to detect the much smaller (37 ppm) ellipsoidal variations in the star HAT P-7 due to its companion, a hot Jupiter in a circular orbit. *Kepler* has also been used to observe dynamical tides in several eccentric binary stars (Thompson et al. 2012). The light curves of these "heartbeat stars" resemble electrocardiograms, with a brightening near periastron and persistent oscillations throughout the orbit. A particularly interesting example is KOI-54 (HD 187091) (Welsh et al. 2011, who also mention three pre-*Kepler* cases). This system contains two very similar A stars in a nearly face-on orbit of eccentricity 0.83 and period 42 days and with a minimum separation of about 6 stellar radii. Fourier analysis of the light curve shows that

several harmonics of the orbital frequency (notably the 90th and 91st) are preferentially excited, as well as some nonharmonic frequencies. Detailed dynamical analyses of this system identify these oscillations as tidally excited g modes in the two stars and reveal evidence for three-mode coupling (Fuller & Lai 2012a, Burkart et al. 2012, O'Leary & Burkart 2014).

5.2. Tidal Evolution in Binary Stars

Indirect evidence of tidal dissipation in stars and giant planets comes from a comparison of the observed distributions of orbital and spin parameters with the expected outcomes of tidal evolution, given reasonable assumptions about the initial conditions. For spectroscopic binary stars, the measured joint distribution of orbital eccentricity e and orbital period P provides good evidence for tidal circularization, showing a clear preference for smaller e at small P. The most detailed study is that of Meibom & Mathieu (2005; see also Mathieu 2005), who plot e versus P for eight populations of solar-type binaries of different ages from pre-main-sequence to late-main-sequence and define a characteristic circularization period (below which orbits are more circular) for each based on a fit to the distribution. The circularization period generally increases with age, suggestive of ongoing tidal dissipation, in a way that is very roughly consistent with $Q' \approx 10^6$ (Ogilvie & Lin 2007; see also Hansen 2010, discussed in Section 5.3 below). It is clear from **Figure 5** that convective damping of the equilibrium tide in a star similar to the present Sun is much too inefficient to explain this result, even with optimistic assumptions ($Q' \approx 10^{10}$ being a more reasonable estimate). (It should be noted that the primary stars span a range of masses around 1 $M_\odot$, and that the secondary stars, which might make an important or even dominant contribution to circularization, are mostly not observed.) If the stars are assumed to be synchronized, then the frequencies of the first-order eccentricity tides (**Table 1**) in the fluid frame are $\hat{\omega} = \pm\Omega_s$ (**Figure 2**) and can excite inertial waves in the convective zone. Studies of the dynamical tide in a solar model can then explain $Q' \approx 10^7$–10^8 (Ogilvie & Lin 2007), but this is still too inefficient to explain the observations. Witte & Savonije (2002) found that the dynamical tide in the radiative zone, together with the effects of rotation and resonant locking, could also provide much more dissipation than the equilibrium tide, but still not enough to explain the observations. A gap still exists, therefore, between theory and observations in this area. [Zahn & Bouchet (1989) previously argued on theoretical grounds that most of the circularization occurs during the pre-main-sequence phase, when the stars are larger and fully convective, but the observations do imply an ongoing process.]

Observations of stellar rotation are more difficult than those of orbital eccentricity, and most diagnose only the rotation of the surface. Meibom et al. (2006) have measured (from periodic photometric variability) the spin periods of the primary stars in several solar-type binaries in two open clusters. Although they do detect two short-period systems with circular orbits and synchronized primaries, their other findings do not appear consistent with the simple expectation that synchronization proceeds much more rapidly than circularization. A partial explanation may be that, as synchronism is approached, the tidal frequency (in the fluid frame) of the asynchronous tide tends to zero, whereas that of the eccentricity tides tends to $\pm\Omega_s$, as noted above. Therefore $\kappa_{2,2,2}$ in Equation 7 tends to zero, and the timescale for synchronization continues to increase, whereas the timescale for circularization tends to a nonzero constant.

For early-type main-sequence stars with radiative envelopes, Khaliullin & Khaliullina (2010) have tested theories of tidal synchronization and circularization in a set of 101 eclipsing binaries, going beyond previous work by Claret & Cunha (1997). Because of concerns that the rotation of the stellar surface might be different from that of the deep interior, they determine the rotation periods using the observed apsidal motion together with theoretical models of stellar structure. After correcting an important numerical error in Khaliullin & Khaliullina (2007), based on a

misreading of Zahn's papers, they find that Zahn's theory of the dynamical tide is compatible with these observations.

For giant stars, success was also found by Verbunt & Phinney (1995), who showed that Zahn's theory of the equilibrium tide, including the effects of stellar evolution, could account for the circularization of spectroscopic binaries containing a giant. The circularization period (more than 200 days) is sufficiently long that the controversial reduction factor for high tidal frequencies is not relevant.

5.3. Tidal Evolution in Extrasolar Planetary Systems

Observations of extrasolar planets by the radial-velocity method allow measurements of the orbital period, the orbital eccentricity, and the "projected" mass of the planet, and observations of transiting planets also provide information on the planetary radius. In some cases the spin period of the star can be measured and its (sky-projected) obliquity (spin-orbit misalignment) determined from the Rossiter-McLaughlin effect; there are no observations yet of the spin periods or obliquities of exoplanets. This is a rapidly developing field that is stimulating interest in tidal interactions. Early applications of tidal theory to exoplanets were made by Rasio et al. (1996), Marcy et al. (1997), and Lubow et al. (1997).

As for binary stars, the clearest evidence for tidal interactions between extrasolar planets and their host stars comes from the joint distribution of orbital eccentricity and orbital period. (Interactive plots of up-to-date exoplanetary data can be generated at **http://exoplanet.eu** or **http://exoplanets.org**.) Orbits of shorter period are more likely to be of low eccentricity (e.g., Kipping 2013). This can be explained by tidal circularization due to dissipation in the planet and is very roughly consistent with $Q'_{\rm p} \approx 10^{6.5}$ (Jackson et al. 2008, Husnoo et al. 2012; but see also Hansen 2010, discussed below). In some systems, especially those with more massive planets such as CoRoT-3, dissipation in the star may also be important for circularization.

As noted in Section 1, in many short-period exoplanetary systems, tidal dissipation in the star leads to inward orbital migration and ultimately to the tidal disruption of the planet rather than to the synchronization of the stellar spin with the orbit as in binary stars. **Figure 10** shows the evolutionary paths (but not the evolutionary timescale) for a planet interacting tidally with a star in the circular, aligned case ($e = i = 0$) in the absence of magnetic braking and other influences. If the total angular momentum L is less than the critical value $L_{\rm c}$ (Equation 1), then the orbit decays and the star is spun up; if $L > L_{\rm c}$, then a stable tidal equilibrium may be approached.

To interpret the observations, we need theories of both planet formation and planet destruction and should perhaps be concerned with the planets that are not observed as much as with those that are. Evidence for inward migration and/or destruction is much less clear than that for circularization. Indeed, the existence of numerous planets in orbits with periods of about 1 d or less implies that the relevant values of Q'_* must greatly exceed the empirical estimate of 10^6 deduced from the circularization of solar-type binary stars; otherwise the remaining lifetimes of the very short-period planets would be implausibly short. An extreme example is WASP-18 b (Hellier et al. 2009), whose remaining lifetime would be about 1×10^6 year if $Q'_* = 10^6$; in this case the orbital decay should be detectable within a few years through transit-time variations (Hellier et al. 2009), although Watson & Marsh (2010) suggest that the effects could be masked by orbital period changes resulting from a variation of the quadrupole moment of the star during its magnetic activity cycle. [Perhaps surprisingly, planets of shorter orbital period such as KOI-1843.03 (Rappaport et al. 2013) and Kepler-78 b (Sanchis-Ojeda et al. 2013) provide a weaker constraint on Q'_* because of the lower planetary masses and higher stellar densities in those systems.] By reexamining the system OGLE-TR-56 b, Adams et al. (2011) have constrained its period derivative

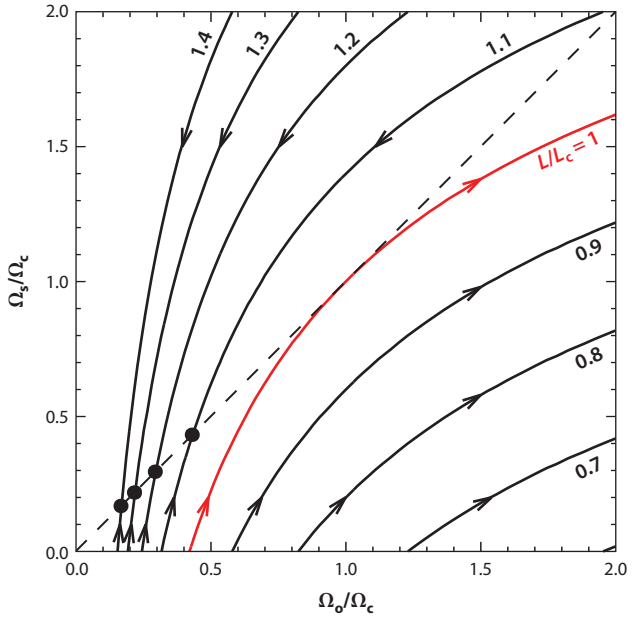

Figure 10

Evolutionary paths for a planet interacting tidally with a star in the circular, aligned case ($e = i = 0$) in the absence of magnetic braking and other influences. The axes represent the (stellar) spin and orbital angular velocities in units of the critical value (Equation 1). Contours of the total angular momentum L are plotted, and the direction of evolution is such that energy is dissipated. The planetary spin is assumed to be unimportant. On the dashed line, the stellar spin is synchronized with the orbit. Black points represent stable tidal equilibria when L exceeds the critical value L_c (Equation 1). Systems with $L < L_c$ evolve toward planetary destruction. The equation of each contour is $(\Omega_s/\Omega_c) + 3(\Omega_o/\Omega_c)^{-1/3} = 4(L/L_c)$.

to be $\dot{P} = -2.9 \pm 17$ ms year^{-1}, i.e., consistent with zero. Their analysis of this result is confusing; in fact, at the 3σ confidence level ($\dot{P} > -54$ ms year^{-1}), it implies that $Q'_* > 1 \times 10^5$.

Despite various attempts to estimate or constrain Q'_* by statistical modeling of the observed orbital semimajor axes and eccentricities, either of populations or of single systems (Jackson et al. 2008, 2009; Hansen 2010; Schlaufman et al. 2010; Brown et al. 2011), there is as yet no convincing evidence of any orbital migration due to tidal dissipation, because the initial conditions are poorly constrained. However, the host stars of several hot Jupiters are said to be spinning faster than expected (Pont 2009, Husnoo et al. 2012), suggesting a tidal transfer of angular momentum from the orbit to the stellar rotation in these systems, and two stars (τ Boo and CoRoT-3) show rotation compatible with synchronization with the orbits of their hot Jupiters (as do KELT-1 and CoRoT-15 with their brown dwarf companions). As mentioned in Section 1, these apparently synchronized systems probably have sufficient total angular momentum to attain a tidal equilibrium. It is not clear what dissipation mechanism can bring this about within the age of the system, though, because these are F stars with shallow convective zones.

Let us recall that Q' is not a fundamental property of a body; even in linear tidal theory, it is expected to depend on the tidal frequency as well as on the integers l and m that label the different spherical harmonics. Even though theory does not yet explain why $Q'_* \approx 10^6$ for the circularization of solar-type binary stars, it can plausibly explain why Q'_* should be much larger for the orbital decay of hot Jupiters. The host stars involved are mostly spinning more slowly than those in close binary stars, and the tidal frequency of the asynchronous tide in the fluid frame is

usually such that $|\hat{\omega}| \gg \Omega_s$. But the eccentricity tides in a synchronized binary star have $|\hat{\omega}| = \Omega_s$ and can excite inertial waves in the convective zone, producing a much stronger tidal response (Ogilvie & Lin 2007). In the radiative zone of a solar-type star, the asynchronous tide can break and produce rapid orbital decay only if the planet and star are sufficiently massive and the star sufficiently old (Barker & Ogilvie 2010; see Section 4.2). The predictions of the wave-breaking theory appear to be in fair agreement with observations (T. Guillot, D.N.C. Lin, P. Morel, in preparation).

The most detailed comparison to date between (highly simplified) tidal theories and exoplanetary observations is that by Hansen (2010, 2012). He evolves interior models of the star and planet, including the effects of tidal heating, together with the equations of tidal evolution of the spin and orbit under the assumption of a common time lag τ, which allows arbitrary eccentricities to be considered. In the first paper (Hansen 2010), he makes the (arbitrary) assumption that all the stars, and all the planets, have fixed values of the parameter (Eggleton et al. 1998)

$$\sigma = \frac{2}{3} k_2 \tau \frac{G}{R^5} = \frac{1}{Q' |\hat{\omega}|} \frac{G}{R^5}. \tag{31}$$

The value of σ_* that he fits from the circularization of solar-type binary stars (see Section 5.2), which corresponds to $Q'_* = 10^6$ in the case of the present Sun for a tidal period of 6 days, would cause much too rapid an evolution of exoplanetary systems, and he finds it necessary to scale it down by more than two orders of magnitude. His preferred value of σ_p corresponds to $Q'_p = 10^8$ in the case of Jupiter for a tidal period of 4 days or to $10^7 \lesssim Q'_p \lesssim 10^8$ for the circularization of hot Jupiters.

In the second paper (Hansen 2012), he instead calculates the value of σ for each star or planet using Zahn's theory of the equilibrium tide, admitting also an empirical correction factor ν_0 for the turbulent viscosity. He finds that a mild correction $\nu_0 \approx 1.5$ is sufficient to explain the circularization of binaries containing a giant star (Verbunt & Phinney 1995) while also being compatible with the nonzero orbital eccentricities of several massive, short-period exoplanets. In fact, as illustrated in **Figure 5**, Zahn's theory is not expected to be applicable to the high tidal frequencies encountered in the latter systems.

Schlaufman & Winn (2013) find evidence for planet destruction by inward migration due to tidal dissipation in subgiant stars. The paucity of planets with $P \lesssim 200$ days around subgiants, in comparison with their presumed main-sequence progenitor stars, is taken as evidence that the shorter-period planets were consumed as the star swelled and developed a deep convective envelope after leaving the main sequence. However, it is difficult to explain the absence of planets out to 200 days by this means unless Q'_* is very small, i.e., of order 10^2 (see also Hansen 2010, 2012).

Measurements of (sky-projected) stellar obliquities provide interesting constraints on scenarios for planet formation, and tidal evolution may play a role in their interpretation. Surprisingly, many systems with hot Jupiters have large spin-orbit misalignments, exceeding 90° in some cases. Winn et al. (2010) argued that most of the cooler stars ($T_{\rm eff} < 6{,}250$ K) are aligned, whereas the hotter stars have widely spread obliquities. They suggested that hot Jupiters are formed in such a way that the stellar obliquities are broadly distributed, but those of the cooler stars are subsequently reduced by tidal dissipation. Albrecht et al. (2012) compiled a set of 53 observed systems and argued that the aligned systems are those in which the timescale for spin-orbit alignment is shorter than the age. They used the estimates by Zahn (1977) for tidal synchronization timescales due to equilibrium and dynamical tides for cooler and hotter stars, respectively. (The alignment timescale might be assumed to be similar to the synchronization timescale in systems for which $L_s \lesssim L_o$; see Equations 7 and 9.) In the case of a planet of 1 Jupiter mass in a 3-day orbit around a star of 1 $M_\odot$

that is slowly rotating with a period of 30 days, the alignment timescale can be estimated roughly as 2,000 Q'_* years, although several different tidal components are potentially involved. Albrecht et al.'s figure 24 (in which they confusingly reduced the timescales by a factor of 5×10^9) suggests, in fact, that tidal alignment is possible within the age of the system for only one or two of the stars, using Zahn's theory of the equilibrium tide.

If stellar tidal dissipation is effective in reducing the obliquity, then there is a danger that the planet will also undergo orbital decay and be destroyed. From Equations 6 and 9 and their generalizations to arbitrary obliquity (e.g., Lai 2012), we can see two situations in which alignment can proceed more rapidly than orbital migration. First, if $L_s \ll L_o$, then alignment can be faster because it involves mainly a change in the stellar spin axis, whereas the orbit is hardly affected. Second, if the tidal response to one or more of the $n = 0$ components (which are associated with a torque but no power, and so do not affect a) is much stronger, then alignment can be accelerated. Indeed, Lai (2012) has noted that the 2, 1, 0 obliquity tide has frequency $\hat{\omega} = -\Omega$ in the fluid frame, within the spectral range of inertial waves, and may thereby elicit a much stronger tidal response. However, Lai (2012) and Rogers & Lin (2013) point out that boosting this component could produce retrograde or even polar orbits, as well as aligned prograde orbits, because the associated di/dt is proportional to $-\sin i \cos^2 i[1 + (L_o/L_s)\cos i]$. Another possible objection is that there is an $m = 1$ mode at exactly $\hat{\omega} = -\Omega$, but it is the spin-over mode rather than a genuine inertial mode and has zero dissipation because it involves a uniform rotation. However, there may be nontrivial dynamics involving a core or involving precessional motion of the spin and orbit due to this secular component of the tidal potential. Further investigation is required.

Transit observations reveal a wide spread of planetary radii, many of which are too large to be explained by conventional models. In principle, tidal dissipation in the planet, due to the synchronization of its spin and the circularization of its orbit, can deposit a very large amount of heat, and the planet can be significantly inflated if the deposition is sufficiently deep. However, this effect does not persist long after the orbit is circularized. Leconte et al. (2010) and Hansen (2010) have concluded that tidal heating cannot provide a general explanation of the radius anomalies.

Nevertheless, Arras & Socrates (2010), following earlier studies of Venus by Gold & Soter (1969) and Correia et al. (2003), have argued that a thermal tide, caused by asymmetric irradiation of the planet by the star, causes a torque that drives the planet away from synchronous spin. The competition between this torque and the gravitational tidal torque could result in a sustained asynchronous state with ongoing tidal dissipation. Although the theory of thermal tides in giant planets is in an embryonic (and controversial) state, A. Socrates (unpublished, arXiv:1304.4121) finds that the expected scaling laws for the resulting tidal heating appear compatible with the observed radius anomalies.

As well as understanding the statistical distributions of properties of extrasolar planets, it is important to consider systems on an individual basis, because of the varying interior structures of stars and planets. Future work ought to take into account the dependence of the tidal response on the extent of a stellar convective zone, for example, or on the size of a planetary core, where this is constrained by observations of the planetary mass and radius.

5.4. Tidal Evolution in the Solar System

Tidal dissipation in the giant planets of the Solar System leads to orbital migration of their regular satellites, which have nearly circular and equatorial orbits. Except for the small, innermost moons that orbit within the planet's corotation radius (synchronous orbit), the migration is outward and its rate is proportional to the mass of the satellite and to the imaginary part of the relevant Love number, $\kappa_{2,2,2}$, at the appropriate tidal frequency. Even without considering the frequency

dependence of the Love number, there is a strong dependence of the migration rate on the orbital separation or period (see Equation 6). Goldreich (1965) proposed that convergent differential migration could cause pairs of satellites to enter the stable commensurabilities (mean-motion resonances) that are observed in numerous cases, including the famous Laplace resonance between Io, Europa, and Ganymede. Two or more satellites that are locked into resonance migrate at a rate determined by their combined angular momentum and the combined tidal torque that the planet exerts on them. Details of the various resonances reveal many interesting puzzles and constraints on tidal dissipation in both the planets and their satellites (Peale 1999).

Goldreich & Soter (1966) deduced lower bounds on the planets' modified tidal quality factors, $Q' = 3/(-2\kappa_{2,2,2})$, from the existence of close satellites (outside corotation), assuming they are as old as the Solar System. It is assumed that Q' does not depend significantly on frequency. The solution for a, starting from $a = a_0$ at $t = t_0$, is then

$$a^{13/2} = a_0^{13/2} + \frac{117}{4}\frac{M_2}{M_1}\frac{R_1^5}{Q'}(GM)^{1/2}(t - t_0). \tag{32}$$

In the case of Jupiter, to move Io alone from the corotation radius to its present location in 4.5×10^9 years requires $Q'_\mathrm{J} = 1.2 \times 10^6$. Once Io, Europa, and Ganymede are locked into resonance, however, their combined angular momentum is 4.3 times that of Io alone, and the combined tidal torque on them is scarcely larger than that on Io alone. This means that Q'_J could be as small as 2.7×10^5 if the resonance is formed early. Combining a similar constraint with a detailed study of the Laplace resonance and the heating of Io, Yoder & Peale (1981) concluded that $2.4 \times 10^5 \lesssim Q'_\mathrm{J} \lesssim 8 \times 10^6$.

In the case of Saturn, to move Mimas alone from the corotation radius to its present location in 4.5×10^9 years requires $Q'_\mathrm{S} = 8.0 \times 10^4$. Once Mimas and Tethys are locked into resonance, however, their combined angular momentum is 22 times that of Mimas alone, and the combined tidal torque on them is 18 times that on Mimas alone (assuming Q'_S is independent of frequency). This means that Q'_S could be as small as 6.6×10^4 if the resonance is formed early.

In the cases of Uranus and Neptune, the existence of Ariel and Proteus provides lower bounds of $Q'_\mathrm{U} \gtrsim 9.1 \times 10^4$ and $Q'_\mathrm{N} \gtrsim 6.7 \times 10^4$, respectively. Based on detailed evolutionary scenarios for Miranda, Ariel, and Umbriel, Tittemore & Wisdom (1990) concluded that $1.6 \times 10^5 \lesssim Q'_\mathrm{U} \lesssim 5.6 \times 10^5$, and most probably toward the lower end of this range.

Recently, however, these constraints have been challenged. Lainey et al. (2009) have fitted a sophisticated dynamical model, including parameterized tidal dissipation, to astrometric observations of the Galilean satellites since 1891, and they deduce $(k_2/Q)_\mathrm{J} = (1.1 \pm 0.2) \times 10^{-5}$, i.e., $Q'_\mathrm{J} = (1.4 \pm 0.3) \times 10^5$, for the asynchronous tide due to Io. This value, which represents only a snapshot of the tidal evolution, is below the lower bounds quoted above for the average over astronomical time and might suggest that Q'_J is in fact frequency dependent.

Applying a similar analysis to Saturn, Lainey et al. (2012) deduce $(k_2/Q)_\mathrm{S} = (2.3 \pm 0.7) \times 10^{-4}$, i.e., $Q'_\mathrm{S} = (7.2 \pm 2.2) \times 10^3$, for the asynchronous tides due to Enceladus, Tethys, Dione, and Rhea. This value is far below the lower bound quoted above, based on the migration of Mimas (and Tethys), and could help to explain the heating rate of Enceladus (cf. Meyer & Wisdom 2007). However, this result is controversial, and Mimas is especially problematic in the model of Lainey et al. because it is apparently migrating inward and would require a large negative torque corresponding to $Q'_\mathrm{S} = -570$. This suggests that the dynamical solution of Lainey et al. may not be correct. The most plausible origin of a negative torque on Mimas's orbit is Tethys, with which it is resonantly locked. It is possible that a nonuniform tidal evolution, due to a strong frequency dependence of Q'_S, could cause the resonant torque between Mimas and Tethys to fluctuate in such a way that Mimas is currently being repelled from Tethys.

The unexpectedly rapid orbital migration deduced by Lainey et al. (2012) has been taken as support for a model in which planetary satellites are formed at the outer edge of a planetary ring system (close to the Roche limit) and migrate outward through a combination of ring torques and planetary tidal torques. Initially, Charnoz et al. (2010) proposed this for the small inner moons (Atlas–Janus) of Saturn. Charnoz et al. (2011) extended this idea to Mimas–Rhea, requiring a small value of Q'_S as suggested by Lainey et al. (2012). (Beyond the 2:1 Lindblad resonance with the outer edge of the rings, only the planetary tidal torque is effective.) However, it has not been demonstrated that the current configuration can be reached while avoiding other stable commensurabilities such as 3:2. More recently, Crida & Charnoz (2012) have applied the same idea to the other planets except Jupiter. For Uranus and Neptune, however, the Roche limit (however reasonably defined) is well inside the corotation radius, and the mechanism may not work; indeed, the inner moons migrate inward and may be disrupted to form rings (Leinhardt et al. 2012).

It is natural to ask what range of values of Q'_S can be explained theoretically and whether Q'_S should be smaller than Q'_J by an order of magnitude or more, as required to cause a significant migration of Saturn's inner moons. The frequency of the asynchronous tide satisfies $|\hat{\omega}/\Omega_s| < 2$ for $0 < \Omega_o/\Omega_s < 2$ (**Figure 2**), which is true for almost all regular satellites. Inertial waves can therefore be excited in the planet. The tidal response can be expected to depend strongly on the tidal frequency and on the size of the core or on other features of the internal structure. Despite considerable uncertainty in the interior models, values of Q' of the right order of magnitude to provide significant tidal evolution of Io and Mimas can certainly be obtained (G.I. Ogilvie, in preparation), and Jupiter's smaller core could explain the difference between the planets. (Models of Uranus and Neptune are even more uncertain at the present time.) An alternative model involving viscoelastic dissipation in the planetary core (Dermott 1979, Remus et al. 2012) could potentially also produce values of Q' of the right order (and strongly increasing with core size, but only weakly dependent on frequency), although the rheological parameters are very uncertain.

We should not be surprised that the values of Q' for giant planets inferred from the orbital migration of their satellites are smaller (perhaps much smaller) than those inferred from the orbital circularization of hot Jupiters, because the tidal frequencies are very different in the two situations. Furthermore, hot Jupiters are expected to be more slowly rotating because of tidal synchronization, and their interiors may differ in an important way from Jupiter and Saturn; the tides in extrasolar planets are also of much larger amplitude and may be in a more nonlinear regime. In both cases the tidal frequency is expected to lie in the spectral range of inertial waves. We have seen that the frequency-averaged response in inertial waves scales such that $Q'^{-1} \propto (\Omega_s/\omega_d)^2$, which naturally provides a difference of about two orders of magnitude between the two situations. The alternative Maxwellian viscoelastic model could potentially explain a difference of about one order of magnitude between the two situations (Storch & Lai 2014), but it also requires that the Maxwell frequency of the core happens to be comparable to the tidal forcing frequencies due to satellites.

SUMMARY POINTS

1. The irreversible evolution of the spin and orbital parameters of an astrophysical fluid body with a close and massive companion is related (at least in the case of uniform rotation) to the rate of dissipation of energy associated with the response of the body to various components of the tidal potential.

2. The response of a fluid body to tidal forcing generally consists of a quasi-hydrostatic bulge and an associated large-scale flow, together with internal (gravity and inertial) waves, often of much smaller scale. Tidal forcing frequencies very often coincide with those of inertial waves.
3. The nonwave-like part of the tide can be dissipated by its interaction with convection or, in some cases, as a result of its own instability or possibly through the action of irreversible effects in multiphase fluids.
4. The wave-like part of the tide has a very different character in radiative and convective zones. Dissipation is effective when the waves achieve a sufficiently small scale to be damped by radiative diffusion or (turbulent) viscosity, when the wave amplitude is enhanced by resonances with global modes, or when nonlinearity causes the waves to break.
5. Idealized calculations of linear tidal responses show a greatly enhanced, but highly frequency-dependent, dissipation rate owing to the excitation of internal waves. Nonideal linear effects and nonlinearity may tend to smooth out the features in the response curves. The evolution of a system with a highly frequency-dependent tidal response is complicated and may involve resonance locking.
6. Tidal dissipation induces differential rotation in fluid bodies, which in turn affects the properties of the internal waves in a way that remains to be fully understood.
7. Observations provide indirect evidence of tidal evolution in binary stars, extrasolar planetary systems, and the satellite systems of the giant planets in the Solar System. In each case useful constraints on theories of tidal dissipation are obtained.

FUTURE ISSUES

1. Further studies of the interaction between oscillatory tidal disturbances and turbulent convection are needed to clarify the role of stellar and planetary convection in tidal dissipation.
2. Linear calculations of the tidal responses of stars and planets should be carried out for a wide range of realistic interior models, including the effects of rotation.
3. Nonlinear aspects of both wave-like and nonwave-like tides should be studied in more detail and under more realistic conditions.
4. The role of differential rotation, and its limitation by various processes inside stars and giant planets, needs to be assessed.
5. Atmospheric tides, both gravitational and thermal, in exoplanets should be studied using specialized numerical simulations.
6. Future observations, especially of transiting exoplanets, are likely to provide improving constraints on theories of tidal dissipation and will require systems to be modeled on an individual basis, taking into account their probable internal structure and evolutionary history.

DISCLOSURE STATEMENT

The author is not aware of any affiliations, memberships, funding, or financial holdings that might be perceived as affecting the objectivity of this review.

ACKNOWLEDGMENTS

I am grateful to Adrian Barker, Harry Braviner, Dong Lai, Doug Lin, John Papaloizou, and Stan Peale for comments and discussions that led to improvements in this review.

LITERATURE CITED

Adams ER, López-Morales M, Elliot JL, et al. 2011. *Ap. J.* 741:102
Aerts C, Christensen-Dalsgaard J, Kurtz DW. 2010. *Asteroseismology*. Dordrecht: Springer
Albrecht S, Reffert S, Snellen I, Quirrenbach A, Mitchell DS. 2007. *Astron. Astrophys.* 474:565–73
Albrecht S, Winn JN Johnson JA, et al. 2012. *Ap. J.* 757:18
Alexander ME. 1973. *Ap. Space Sci.* 23:459–510
Arras P, Socrates A. 2010. *Ap. J.* 714:1–12
Barker AJ. 2011. *MNRAS* 414:1365–78
Barker AJ, Lithwick Y. 2013a. *MNRAS* 435:3614–26
Barker AJ, Lithwick Y. 2013b. *MNRAS* 437:305–15
Barker AJ, Ogilvie GI. 2010. *MNRAS* 404:1849–68
Baruteau C, Rieutord M. 2013. *J. Fluid Mech.* 719:47–81
Bildsten L, Cutler C. 1992. *Ap. J.* 400:175–80
Bodenheimer P, Lin DNC, Mardling RA. 2001. *Ap. J.* 548:466–72
Bouchy F, Deleuil M, Guillot T. 2011. *Astron. Astrophys.* 525:A68
Brown DJA, Collier Cameron A, Hall C, Hebb L, Smalley B. 2011. *MNRAS* 415:605–18
Bryan GH. 1889. *Philos. Trans. R. Soc. Lond. A* 180:187–219
Burkart J, Quataert E, Arras P, Weinberg NN. 2012. *MNRAS* 421:983–1006
Cartan E. 1922. *Bull. Sci. Math. France* 46:317–52
Cartwright DE. 1999. *Tides: A Scientific History*. Cambridge: Cambridge Univ. Press
Cébron D, Le Bars M, Le Gal P, et al. 2013. *Icarus* 226:1642–53
Cébron D, Le Bars M, Leontini J, Maubert P, Le Gal P. 2010. *Phys. Earth Planet. Inter.* 182:119–28
Charnoz S, Crida A, Castillo-Rogez JC, et al. 2011. *Icarus* 216:535–50
Charnoz S, Salmon J, Crida A. 2010. *Nature* 465:752–54
Claret A, Cunha NCS. 1997. *Astron. Astrophys.* 318:187–97
Comeau S, Poisson E. 2009. *Phys. Rev. D* 80:087501
Correia ACM, Laskar J, Néron de Surgy O. 2003. *Icarus* 163:1–23
Counselman CC. 1973. *Ap. J.* 180:307–16
Cowling TG. 1941. *MNRAS* 101:367–75
Crida A, Charnoz S. 2012. *Science* 338:1196–99
Darwin GH. 1880. *Philos. Trans. R. Soc. Lond.* 171:713–891
Deparis V, Legros H, Souchay J. 2013. In *Tides in Astronomy and Astrophysics*, ed. J Souchay, S Mathis, T Tokieda, pp. 31–82. Heidelberg: Springer
Dermott SF. 1979. *Icarus* 37:310–21
Dintrans B, Rieutord M, Valdettaro L. 1999. *J. Fluid Mech.* 398:271–97
Eckart C. 1960. *Hydrodynamics of Oceans and Atmospheres*. Oxford: Pergamon
Eggleton PP, Kiseleva LG, Hut P. 1998. *Ap. J.* 499:853–70
Fabian AC, Pringle JE, Rees MJ. 1975. *MNRAS* 172:15p–18p
Favier B, Barker AJ, Baruteau C, Ogilvie GI. 2014. *MNRAS* 493:845–60
French M, Becker A, Lorenzen W, et al. 2012. *Ap. J. Suppl.* 202:5
Fuller J, Lai D. 2012a. *MNRAS* 420:3126–38

Fuller J, Lai D. 2012b. *MNRAS* 421:426–45
Gavrilov SV, Zharkov VN. 1977. *Icarus* 32:443–49
Giersz M. 1986. *Acta Astron.* 36:181–209
Gold T, Soter S. 1969. *Icarus* 11:356–66
Goldreich P. 1963. *MNRAS* 126:257–68
Goldreich P. 1965. *MNRAS* 130:159–81
Goldreich P, Keeley DA. 1977. *Ap. J.* 211:934–42
Goldreich P, Nicholson PD. 1977. *Icarus* 30:301–4
Goldreich P, Nicholson PD. 1989. *Ap. J.* 342:1079–84
Goldreich P, Soter S. 1966. *Icarus* 5:375–89
Goodman J, Dickson ES. 1998. *Ap. J.* 507:938–44
Goodman J, Lackner C. 2009. *Ap. J.* 696:2054–67
Goodman J, Oh SP. 1997. *Ap. J.* 486:403–12
Greenspan H. 1968. *The Theory of Rotating Fluids*. Cambridge: Cambridge Univ. Press
Gu P-G, Lin DNC, Bodenheimer PH. 2003. *Ap. J.* 588:509–34
Guillochon J, Ramirez-Ruiz E, Lin D. 2011. *Ap. J.* 732:74
Hansen BMS. 2010. *Ap. J.* 723:285–99
Hansen BMS. 2012. *Ap. J.* 757:6
Hartle JB. 1973. *Phys. Rev. D* 8:1010–24
Hebb L, Collier Cameron A, Triaud AHMJ, et al. 2010. *Ap. J.* 708:224–31
Hellier C, Anderson DR, Collier Cameron A, et al. 2009. *Nature* 460:1098–100
Hough SS. 1897. *Philos. Trans. R. Soc. Lond. A* 189:201–57
Hough SS. 1898. *Philos. Trans. R. Soc. Lond. A* 191:139–85
Husnoo N, Pont F, Mazeh T, et al. 2012. *MNRAS* 422:3151–77
Hut P. 1980. *Astron. Astrophys.* 92:167–70
Hut P. 1981. *Astron. Astrophys.* 99:126–40
Ibgui L, Burrows A. 2009. *Ap. J.* 700:1921–32
Ioannou PJ, Lindzen RS. 1993. *Ap. J.* 406:266–78
Ivanov PB, Papaloizou JCB. 2007. *MNRAS* 376:682–704
Ivanov PB, Papaloizou JCB. 2010. *MNRAS* 407:1609–30
Jackson B, Barnes R, Greenberg R. 2009. *Ap. J.* 698:1357–66
Jackson B, Greenberg R, Barnes R. 2008. *Ap. J.* 678:1396–406
Jeffreys H. 1961. *MNRAS* 122:339–43
Jouve L, Ogilvie GI. 2014. *J. Fluid Mech.* 745:223–50
Kaula WM. 1961. *Geophys. J. Int.* 5:104–33
Kerswell RR. 2002. *Annu. Rev. Fluid Mech.* 34:83–113
Khaliullin KhF, Khaliullina AI. 2007. *MNRAS* 382:356–66
Khaliullin KhF, Khaliullina AI. 2010. *MNRAS* 401:257–74
Kipping D. 2013. *MNRAS* 434:L51–55
Kochanek CS. 1992. *Ap. J.* 398:234–47
Kopal Z. 1978. *Dynamics of Close Binary Systems*. Dordrecht: Reidel
Kosovichev AG, Novikov ID. 1992. *MNRAS* 258:715–24
Kramm U, Nettelmann N, Fortney JJ, Neuhaüser R, Redmer R. 2012. *Astron. Astrophys.* 538:A146
Kumar P, Goodman J. 1996. *Ap. J.* 466:946–56
Lai D. 1997. *Ap. J.* 490:847–62
Lai D. 2012. *MNRAS* 423:486–92
Lainey V, Arlot J-E, Karatekin Ö, van Hoolst T. 2009. *Nature* 459:957–59
Lainey V, Karatekin Ö, Desmars J, et al. 2012. *Ap. J.* 752:14
Langer N. 2009. *Astron. Astrophys.* 500:133–34
Laplace PS. 1775. *Mém. Acad. R. Sci.* 88:75–182
Le Bars M, Lacaze L, Le Dizès S, Le Gal P, Rieutord R. 2010. *Phys. Earth Planet. Inter.* 178:48–55
Leconte J, Chabrier G, Baraffe I, Levrard B. 2010. *Astron. Astrophys.* 516:A64
Lee HM, Ostriker JP. 1986. *Ap. J.* 310:176–88

Leinhardt ZM, Ogilvie GI, Latter HN, Kokubo E. 2012. *MNRAS* 424:1419–31
Levrard B, Winisdoerffer C, Chabrier G. 2009. *Ap. J. Lett.* 692:L9–13
Lubow SH, Tout CA, Livio M. 1997. *Ap. J.* 484:866–70
Maas LRM, Lam F-PA. 1995. *J. Fluid Mech.* 300:1–41
McMahon JM, Morales MA, Pierleoni C, Ceperley DM. 2012. *Rev. Mod. Phys.* 84:1607–53
McMillan SLW, McDermott PN, Taam RE. 1987. *Ap. J.* 318:261–77
Marcy GW, Butler RP, Williams E, et al. 1997. *Ap. J.* 481:926–35
Mardling RA. 1995a. *Ap. J.* 450:722–31
Mardling RA. 1995b. *Ap. J.* 450:732–47
Mathieu RD. 2005. In *Tidal Evolution and Oscillations in Binary Stars: Third Granada Workshop on Stellar Structure*, ed. A Claret, A Giménez, J-P Zahn. *ASP Conf. Ser.* 333:26–38. San Francisco: ASP
Matsumura S, Peale SJ, Rasio FA. 2010. *Ap. J.* 725:1995–2016
Meibom S, Mathieu RD. 2005. *Ap. J.* 620:970–83
Meibom S, Mathieu RD, Stassun KG. 2006. *Ap. J.* 653:621–35
Meyer J, Wisdom J. 2007. *Icarus* 188:535–39
Mied RP. 1976. *J. Fluid Mech.* 78:763–84
Ogilvie GI. 2005. *J. Fluid Mech.* 543:19–44
Ogilvie GI. 2009. *MNRAS* 396:794–806
Ogilvie GI. 2013. *MNRAS* 429:613–32
Ogilvie GI, Lesur G. 2012. *MNRAS* 422:1975–87
Ogilvie GI, Lin DNC. 2004. *Ap. J.* 610:477–509
Ogilvie GI, Lin DNC. 2007. *Ap. J.* 661:1180–91
O'Leary RM, Burkart J. 2014. *MNRAS* 440:3036–50
Papaloizou JCB, Ivanov PB. 2005. *MNRAS* 364:L66–70
Papaloizou JCB, Ivanov PB. 2010. *MNRAS* 407:1631–56
Papaloizou JCB, Pringle JE. 1978. *MNRAS* 182:423–42
Papaloizou JCB, Savonije GJ. 1997. *MNRAS* 291:651–57
Peale SJ. 1999. *Annu. Rev. Astron. Astrophys.* 37:533–602
Penev K, Barranco J, Sasselov D. 2009a. *Ap. J.* 705:285–97
Penev K, Sasselov D, Robinson F, Demarque P. 2007. *Ap. J.* 655:1166–71
Penev K, Sasselov D, Robinson F, Demarque P. 2009b. *Ap. J.* 704:930–36
Poincaré H. 1885. *Acta Math.* 7:259–380
Poisson E. 2009. *Phys. Rev. D* 80:064029
Polfliet R, Smeyers P. 1990. *Astron. Astrophys.* 237:110–24
Pont F. 2009. *MNRAS* 396:1789–96
Press WH, Teukolsky SA. 1977. *Ap. J.* 213:183–92
Press WH, Wiita PJ, Smarr LL. 1975. *Ap. J. Lett.* 202:L135–37
Rappaport S, Sanchis-Ojeda R, Rogers LA, Levine A, Winn JN. 2013. *Ap. J. Lett.* 773:L15
Rasio FA, Tout CA, Lubow SH, Livio M. 1996. *Ap. J.* 470:1187–91
Remus F, Mathis S, Zahn J-P, Lainey V. 2012. *Astron. Astrophys.* 541:A165
Rieutord M. 1992. *Astron. Astrophys.* 259:581–84
Rieutord M. 2004. In *Stellar Rotation*, *Proc. IAU Symp. 215*, ed. A Maeder, PRJ Eenens, pp. 394–403. San Francisco: ASP
Rieutord M, Georgeot B, Valdettaro L. 2001. *J. Fluid Mech.* 435:103–44
Rieutord M, Valdettaro L. 2010. *J. Fluid Mech.* 643:363–94
Rieutord M, Zahn J-P. 1997. *Ap. J.* 474:760–67
Rogers TM, Lin DNC. 2013. *Ap. J. Lett.* 769:L10
Sanchis-Ojeda R, Rappaport S, Winn JN, et al. 2013. *Ap. J.* 774:54
Savonije GJ, Papaloizou JCB. 1983. *MNRAS* 203:581–93
Savonije GJ, Papaloizou JCB. 1984. *MNRAS* 207:685–704
Savonije GJ, Papaloizou JCB. 1997. *MNRAS* 291:633–50
Savonije GJ, Papaloizou JCB, Alberts F. 1995. *MNRAS* 277:471–96
Savonije GJ, Witte MG. 2002. *Astron. Astrophys.* 386:211–21

Schlaufman KC, Lin DNC, Ida S. 2010. *Ap. J. Lett.* 724:L53–58
Schlaufman KC, Winn JN. 2013. *Ap. J.* 772:143
Siverd RJ, Beatty TG, Pepper J, et al. 2012. *Ap. J.* 761:123
Sridhar S, Tremaine S. 1992. *Icarus* 95:86–99
Stevenson DJ. 1983. *J. Geophys. Res.* 88:2445–55
Storch NI, Lai D. 2014. *MNRAS* 438:1526–34
Tassoul J-L. 1987. *Ap. J.* 322:856–61
Terquem C, Papaloizou JCB, Nelson RP, Lin DNC. 1998. *Ap. J.* 502:788–801
Thompson SE, Everett M, Mullally F, et al. 2012. *Ap. J.* 753:86
Thomson W. 1863. *Philos. Trans. R. Soc. Lond.* 153:583–616
Thomson W. 1880. *Philos. Mag.* 10:155–68
Thorne KS, Price RH, MacDonald DA. 1986. *Black Holes: The Membrane Paradigm*. New Haven: Yale Univ. Press
Tittemore WC, Wisdom J. 1990. *Icarus* 85:394–443
Venumadhav T, Zimmerman A, Hirata CM. 2014. *Ap. J.* 781:23
Verbunt F, Phinney ES. 1995. *Astron. Astrophys.* 296:709–21
Watson CA, Marsh TR. 2010. *MNRAS* 405:2037–43
Weinberg NN, Arras P, Burkart J. 2013. *Ap. J.* 769:121
Weinberg NN, Arras P, Quataert E, Burkart J. 2012. *Ap. J.* 751:136
Welsh WF, Orosz JA, Aerts C, et al. 2011. *Ap. J. Suppl.* 197:4
Welsh WF, Orosz JA, Seager S, et al. 2010. *Ap. J. Lett.* 713:L145–49
Winn JN, Fabrycky D, Albrecht S, Johnson JA. 2010. *Ap. J. Lett.* 718:L145–49
Witte MG, Savonije GJ. 1999a. *Astron. Astrophys.* 341:842–52
Witte MG, Savonije GJ. 1999b. *Astron. Astrophys.* 350:129–47
Witte MG, Savonije GJ. 2001. *Astron. Astrophys.* 366:840–57
Witte MG, Savonije GJ. 2002. *Astron. Astrophys.* 386:222–36
Wu Y. 2005a. *Ap. J.* 635:674–87
Wu Y. 2005b. *Ap. J.* 635:688–710
Yoder CF, Peale SJ. 1981. *Icarus* 47:1–35
Zahn J-P. 1966a. *Ann. Astrophys.* 29:313–30
Zahn J-P. 1966b. *Ann. Astrophys.* 29:489–506
Zahn J-P. 1970. *Astron. Astrophys.* 4:452–61
Zahn J-P. 1975. *Astron. Astrophys.* 41:329–44
Zahn J-P. 1977. *Astron. Astrophys.* 57:383–94
Zahn J-P. 1989. *Astron. Astrophys.* 220:112–16
Zahn J-P, Bouchet L. 1989. *Astron. Astrophys.* 223:112–18

Annual Review of Astronomy and Astrophysics

Volume 52, 2014

Contents

Indexes

Errata

An online log of corrections to *Annual Review of Astronomy and Astrophysics* articles may be found at http://www.annualreviews.org/errata/astro